Rep. Prog. Phys. 56 (1993) 1347–1395. Printed in the UK

# Numerical simulations in particle physics

Frithjof Karsch†‡ and Edwin Laermann‡
† HLRZ, c/o KFA Jülich, D-52425 Jülich, Federal Republic of Germany
‡ Fakultät für Physik, Universität Bielefeld, D-33615 Bielefeld 1, Federal Republic of Germany

## Abstract

Numerical simulations have become an important tool to understand and predict non-perturbative phenomena in particle physics. In this article we attempt to present a general overview over the field. First, the basic concepts of lattice gauge theories are described, including a discussion of currently used algorithms and the reconstruction of continuum physics from lattice data. We then proceed to present some results for QCD, both at low energies and at high temperatures, as well as for the electro-weak sector of the standard model.

This review was received in April 1993.

0034-4885/93/111347 + 49$30.00  

**Contents**

## 1. Introduction

There is a general belief among particle physicists that the fundamental forces in physics are described by quantum field theories (QFTs) with local gauge invariance. Although, at present, there does not exist a satisfactory framework for the inclusion of the gravitational force, the remaining electromagnetic, weak and strong forces have been combined in a unified model—the standard model. The standard model is based on three symmetry groups, $U(1)$ and $SU(2)$ for electromagnetism and weak isospin and colour $SU(3)$. These theories have been tested experimentally and at least in the perturbative regime the theoretical predictions have been found to be in remarkable agreement with experiment. However, these theories also incorporate many important non-perturbative concepts, like confinement, spontaneous chiral symmetry breaking or the Higgs mechanism. These properties lead to drastic consequences for the spectrum of these theories as well as for their phase structure at non-zero temperature. The quantitative study of such non-perturbative aspects of a QFT, e.g. a determination of the mass spectrum or the location of a phase transition, in a perturbative context is rather limited and non-perturbative approaches are needed to make any progress in a quantitative analysis of the consequences of these crucial features of a QFT.

The exploration of field theories and the study of their non-perturbative structure received new impetus in the 70s through a newly developed regularization scheme for the singularities of QFTs—the lattice regularization. The formulation of lattice regularized field theories (Wilson 1974) has put the connection between the Euclidean path integral formulation of QFTs and statistical models on 4-dimensional lattices on a solid footing. It immediately opened the possibility for applying standard methods from statistical physics, which have been used there for many years, to the analysis of QFTs.

Naturally these new lattice models first have been studied using the well developed high and low temperature series expansion techniques known in statistical physics (Drouffe and Itzykson 1978). However, it was an obvious step also to attempt to apply Monte Carlo simulation techniques (Binder 1979) to the rather complex field theoretic models, once the computers were powerful enough to lead to statistically significant results within a reasonable time scale. Indeed the first results from such numerical studies were exciting (Creutz 1980 and for a collection of early results see also Rebbi 1983) and led to the hope that long standing non-perturbative questions, like the confinement problem in QCD, could be answered quantitatively this way. In fact, these first studies paved the way for a new branch in theoretical high energy physics—lattice field theory.

Numerical studies are nowadays used to explore the structure of almost all quantum field theories of interest, ranging from 2-dimensional spin models to the basic building blocks of our standard model for the fundamental forces in nature (Creutz 1992). In particular in the analysis of quantum chromodynamics (QCD) much progress has been made towards a quantitative determination of such fundamental properties of the theory as its particle spectrum, the strength of the confinement force and the phase structure at finite temperature, although the required computer resources became much larger than originally anticipated. In fact, today several groups working in the field decided to develop dedicated machines for their projects (Marinari 1993) and there even exist advanced plans for the construction of massively parallel, dedicated computers with Teraflops performance (Christ 1990, Negele 1993). Consequently a good fraction of research activities in the context of lattice field theories today is spent in the development of new simulation techniques. Substantial progress has been made here for purely bosonic field theories, where cluster and multigrid algorithms led to much improved simulation techniques. Crucial for the simulation of the standard model, however, is the handling of fermions. Finding faster algorithms for the

fermionic sector of a QFT will be vital for future progress in this field (Herrmann and Karsch 1991, Creutz 1992).

In this paper we will describe some of the basic algorithms used for the simulation of lattice field theories and review basic results that emerged from these simulations. Although our notation is oriented towards applications in the analysis of QCD, it applies, with minor modifications, to other sectors of the standard model. We will discuss in the next section fundamental concepts in the formulation of lattice field theories, putting emphasis on the currently used simulation techniques and the reconstruction of continuum physics from lattice calculations. In the following sections some basic results are discussed. In these sections we will, wherever possible, try to avoid going into a description of technical details of the actual Monte Carlo simulations. Sections 3 and 4 are devoted to a presentation of results obtained from simulations of QCD. In section 3 we discuss results on the low energy physics, while section 4 deals with the finite temperature phase transition and the physics of the quark–gluon plasma. Similarly we discuss in section 5 the zero and finite temperature physics of the electro-weak sector of the standard model on the lattice. Finally we give an outlook on future developments in section 6.

## 2. Particle physics on the lattice

### *2.1. Lattice regularized quantum field theory*

Almost all numerical studies of quantum field theories (QFTs) are based on the Euclidean path integral formulation of these theories. The vacuum to vacuum transition amplitude is given as a path integral over all Euclidean field configurations

$$Z_E = \int \mathcal{D}\Phi e^{-S_E} \tag{2.1}$$

where $S_E$ is the Euclidean action, which defines the QFT in terms of a 4-dimensional integral over the Lagrangian, $\mathcal{L}$,

$$S_E = \int d^4x\, \mathcal{L}(\Phi). \tag{2.2}$$

The Lagrangian depends only on the fundamental fields $\Phi(t,\mathbf{x})$ and a set of coupling constants. Information on the spectrum, as well as various other properties of the theory, can be obtained from the behaviour of $n$-point Green functions,

$$G(x_1, x_2, \ldots, x_n) = Z_E^{-1} \int \mathcal{D}\Phi \Phi(x_1)\Phi(x_2)\ldots\Phi(x_n) e^{-S_E}. \tag{2.3}$$

For example, the mass $m_\Phi$ of a particle created by the field $\Phi$ can be computed from the exponential decrease of the two-point function at large time separations $t$,

$$\langle \Phi(t)\Phi(0)\rangle \xrightarrow{t\to\infty} Z_\Phi \exp(-m_\Phi t), \tag{2.4}$$

where $Z_\Phi$ is the usual wave-function renormalization.

It is quite straightforward to generalize the path integral formulation of a QFT to finite temperature (and chemical potential) (Bernard 1974). The temperature and volume of a thermodynamic system enter through the restriction of the fundamental fields to a finite $(3+1)$-dimensional region of space-time. In particular, the temperature, $T$, enters by restricting

the Euclidean time interval to the range $t \in [0, 1/T]$ and by demanding periodic (anti-periodic) boundary conditions for bosonic (fermionic) fields in this direction,

$$Z(V, T) = \int \mathscr{D}\Phi e^{-S_E(V,T)} \tag{2.5}$$

with

$$S_E(V, T) = \int_0^{1/T} dx_0 \int_V d^3x \, \mathscr{L}(\Phi). \tag{2.6}$$

Thermodynamic quantities can then be obtained as derivatives of the partition function $Z(V, T)$. For instance, the energy density and the pressure are given by

$$\epsilon = \frac{T^2}{V} \frac{\partial}{\partial T} \ln Z, \qquad p = T \frac{\partial}{\partial V} \ln Z. \tag{2.7}$$

A QFT, defined formally by the above relations, needs to be regularized in order to give a meaning to the path-integral and to remove ultraviolet divergencies in the theory. This can be done by introducing a cut-off in coordinate (or momentum) space. A renormalization scheme, which allows to remove the cut-off again, can then be defined and allows to separate divergent parts from the physical, finite sector. For the purpose of numerical studies of QFTs the introduction of a discrete space-time lattice is the most convenient regularization scheme. It reduces the number of degrees of freedom to a large but finite set and gives a well defined statistical interpretation to the path integral and most observables of interest, which can be viewed as expectation values calculated in a statistical ensemble with Boltzmann weights $\exp(-S_E)$.

On a 4-dimensional spacetime lattice with a lattice spacing '$a$', the fields $\Phi(x)$ are restricted to the discrete set of points, $(x_0, \mathbf{x}) \to na \equiv (n_0 a, n_1 a, n_2 a, n_3 a)$. Accordingly, $\Phi(x)$ gets replaced by $\phi(n)$ and the measure in the path integral becomes, $\mathscr{D}\Phi \to \Pi_n d\phi(n)$. A finite, 4-dimensional lattice of size $N_\tau \times N_\sigma^3$ does then represent a statistical system at temperature $T = 1/N_\tau a$ in a volume of size $V = (N_\sigma a)^3$. The partition function of this system reads

$$Z_E = \int \prod_n d\phi(n) e^{-S_E(V,T)}. \tag{2.8}$$

The crucial step in formulating a lattice regularized QFT is the proper discretization of the Euclidian action, $S_E$. This can be achieved in a straightforward way for a scalar field theory by discretizing the integral in (2.6) and replacing derivatives of fields by finite differences. The action of the $\phi^4$-theory for instance, may be discretized as

$$\begin{aligned} &\int d^4x \Big\{ \frac{1}{2} (\partial\Phi(x))^2 + \frac{1}{2} m_0^2 \Phi^2(x) + \frac{g_0}{4!} \Phi^4(x) \Big\} \\ &\to \sum_{n=(n_0,\ldots,n_3)} \Big\{ -2\kappa \sum_{\mu=0}^{3} \phi(n)\phi(n + \hat{\mu}) + \lambda[\phi^2(n) - 1]^2 + \phi^2(n) \Big\}. \end{aligned} \tag{2.9}$$

with $\hat{\mu}$ denoting the unit vector pointing to neighbouring sites in a 4-dimensional lattice and $\kappa$, $\lambda$ are couplings, which in the naive continuum limit, $a \to 0$, are related to $m_0$, $g_0$ as $g_0 = 6\lambda/\kappa^2$, $m_0^2 = (1 - 2\lambda - 8\kappa)/\kappa$.

In the case of a gauge theory the discretization is not at all so obvious. In fact, it is important to choose a discretization such that the basic symmetries of the continuum action

are preserved. This is not always possible as we will see from our discussion of fermionic theories. However, the most important step clearly is to construct a discretized action which preserves local gauge invariance. Wilson has shown first how one can achieve this (Wilson 1974).

*2.1.1. Gauge fields on the lattice.* Gauge fields mediate the interactions between matter. It is thus suggestive to introduce them as variables on the links $(n, \mu)$ of a hypercubic, 4-dimensional lattice rather than on the sites of the lattice. Gauge fields, $\mathscr{A}_\mu(x)$, can then be related to elements $U_\mu(n)$ of a gauge group. To be specific we will consider the case of an $SU(N)$ gauge theory, which is relevant for the formulation of QCD as well as the $SU(2)$-Higgs model†. On a lattice with lattice spacing $a$ the formal relation between $U_\mu(n)$ and $\mathscr{A}_\mu(x)$ is given by

$$U_\mu(n) = \exp\left[-iga \sum_{b=1}^{N^2-1} \lambda^b \mathscr{A}^b_\mu(x)\right] \tag{2.10}$$

where $g$ is the bare coupling constant and $\lambda^b$ are the generators of the group. Using this relation one can easily verify that the single plaquette action proposed by Wilson

$$S_G = \frac{2N}{g^2} \sum_{n;0\leqslant\mu<\nu\leqslant 3} P_{\mu\nu}(n) \tag{2.11}$$

with

$$P_{\mu\nu}(n) = 1 - \frac{1}{N} \mathrm{Re}\,\mathrm{Tr}\, U_\mu(n) U_\nu(n+\hat{\mu}) U_\mu^{-1}(n+\hat{\nu}) U_\nu^{-1}(n) \tag{2.12}$$

approximates the continuum Lagrangian for the gauge fields up to terms of $O(a^6)$, $(2N/g^2)P_{\mu\nu}(n) = \frac{1}{4}a^4 F^b_{\mu\nu} F^b_{\mu\nu} + O(a^6)$. In the continuum limit, $a \to 0$, these higher order corrections become irrelevant.

*2.1.2. Fermions on the lattice.* Wilson also suggested a discretization scheme for fermionic actions. While it is easy to preserve local gauge invariance also in this case, it is difficult to preserve all the chiral properties of fermionic actions. Fermion actions contain only first derivatives of the fields. As a consequence, a straightforward discretization, similar to the scalar case described in (2.9), leads to additional poles in the lattice fermion propagator. In the continuum limit these additional poles will give rise to 15 additional, unwanted fermion species rather than only the one we started with. It could be observed (Nielsen and Ninomiya 1981) that this is a general phenomenon when in addition to such elementary assumptions as locality, hermiticity and translational invariance also a continuous chiral symmetry of the action is required. There are however certain loopholes. Wilson proposed a discretization scheme for fermions, in which a second-order derivative term $S_W$ is added to the naively discretized fermion action $S_F$,

$$\begin{aligned} S_{WF} &= S_F + S_W \\ &= \frac{1}{2} \sum_{x,\mu} \{\bar{\psi}(x)\gamma_\mu \psi(x+\hat{\mu}) - \bar{\psi}(x+\hat{\mu})\gamma_\mu \psi(x)\} \\ &\quad + \frac{1}{2} \sum_{x,\mu} \{2\bar{\psi}(x)\psi(x) - \bar{\psi}(x+\hat{\mu})\psi(x) - \bar{\psi}(x)\psi(x+\hat{\mu})\}. \end{aligned} \tag{2.13}$$

† The following discussion, of course, can easily be reformulated for an abelian gauge theory like $U(1)$.

The additional term $S_W$ becomes irrelevant in the (naive) continuum limit. Its effect is that the 15 additional fermions acquire a large mass of $O(1/a)$, which diverges in the continuum limit, and thus would decouple from the dynamics of the theory. However, chiral invariance of the action is lost at finite lattice spacing and is to be recovered in the continuum limit.

Another approach, which we want to discuss in the following is due to Kogut and Susskind (Kogut and Susskind 1975). By distributing the four components of the continuum spinor over different sites of the lattice it is possible to reduce the number of additional species. If one introduces $\tilde{f}$ different staggered fermion species on the lattice the staggered lattice action will lead to $n_f = 4\tilde{f}$ species of fermions in the continuum limit. Moreover it preserves a global $U(\tilde{f}) \times U(\tilde{f})$ chiral symmetry, i.e. an abelian subgroup of the continuum chiral symmetry. For studies of chiral symmetry breaking as well as for finite temperature calculations on the lattice it is convenient to work with such a lattice action which preserves at least part of the $SU(n_f) \times SU(n_f)$ chiral symmetry of the continuum action. The staggered fermion action, obtained after a diagonalization in the Dirac indices, becomes

$$S_F = \sum_{i=1}^{\tilde{f}} \sum_{n,m} \bar{\chi}_i(n) Q^i(n, m) \chi_i(m). \tag{2.14}$$

Here the fermion fields, $\chi$, $\bar{\chi}$, are anticommuting Grassmann variables defined on the sites of the lattice and the fermion matrix $Q_i(n, m)$ is given by

$$Q^i(n, m) = \sum_{\mu=0}^{3} D_\mu(n, m) + m_i \delta(n, m). \tag{2.15}$$

The hopping matrices $D_\mu(n,m)$ mediate the nearest neighbour interactions and have non-zero elements only for $m = n \pm \hat{\mu}$,

$$D_\mu(n, m) = \frac{1}{2} \eta_\mu(n) [U_\mu(n) \delta(n, m - \hat{\mu}) - U_\mu^{-1}(n) \delta(n, m + \hat{\mu})]. \tag{2.16}$$

The phase factors $\eta_\mu(n) = (-1)^{n_0 + \cdots + n_{\mu-1}}$ for $\mu > 0$ and $\eta_0 = 1$ are remnants of the $\gamma_\mu$ matrices. Finally the partition function takes on the form

$$Z = \int \prod_{n,\mu} dU_\mu(n) \prod_{n,i} d\chi_i(n) d\bar{\chi}_i(n) e^{[-S_G - S_F]}. \tag{2.17}$$

As the fermionic part of the action is bilinear in the fields $\bar{\chi}_i(n)$, $\chi_i(n)$, these can be integrated out and the partition function can be represented in terms of bosonic degrees of freedom only,

$$Z = \int \prod_{n,\mu} dU_\mu(n) \prod_{i=1}^{\tilde{f}} \det Q^i e^{-S_G}. \tag{2.18}$$

In this form the partition function is well suited for numerical studies. A major problem is, however, caused by the presence of the fermion determinant, which in general cannot be calculated exactly. Algorithms for the numerical integration are thus required, which circumvent the explicit calculation of this determinant.

### *2.2. Numerical simulations*

*2.2.1. Basic concepts: Metropolis and heat bath algorithm.* In the lattice regularization, the Feynman path integral, (2.8), becomes a well-defined meaning as an ordinary integral. Because of the high-dimensionality, its numerical evaluation, however, is a formidable task. *Imagine a lattice of just $10^4$ lattice points, then (2.8) represents a $10^4$ fold integral times the* number of internal degrees of freedom. Many field configurations $\{\phi\}$ will contribute to the integral with rather small Boltzmann weights, $\exp\{-S(\phi)\}$, though. Thus an efficient way to compute the integral would consist in generating a sequence of field configurations $\{\phi\}^{(k)}$ which are distributed according to this weight factor. The expectation value of an observable $\mathcal{O}(\phi)$ can then be approximated by the ensemble average

$$\langle \mathcal{O}(\phi) \rangle = \frac{1}{M} \sum_{k=1}^{M} \mathcal{O}(\phi)^{(k)}. \tag{2.19}$$

Such a series of field configurations is obtained by means of so-called Markov chains. Starting from some arbitrary initial configuration $\{\phi(n)\}^{(0)}$ one generates, one after the other, new sets of $\phi$ fields. Under certain conditions, the sets $\{\phi\}^{(k)}$ will be distributed according to the equilibrium probability $\exp\{-S(\phi)\}$, once a number of not-yet equilibrated initial configurations has been discarded.

The prototype algorithm which meets these conditions is the Metropolis algorithm (Metropolis *et al* 1953). It consists of two steps: site by site (i) choose a trial update $\phi'$ according to some normalized probability distribution $P_{\text{trial}}(\phi \to \phi') = P_{\text{trial}}(\phi' \to \phi)$ and (ii) accept $\phi'$ with the conditional probability

$$P_{\text{accept}} = \min\left\{1, \frac{e^{-S(\phi')}}{e^{-S(\phi)}}\right\}. \tag{2.20}$$

The trial distribution $P_{\text{trial}}$ must be chosen in such a way that the whole configuration space can be covered. The conditional accept probability $P_{\text{accept}}$ allows for configurations with a smaller Boltzmann weight to be included in the set. This is necessary in order to account for the quantum fluctuations. Finally, the algorithm satisfies detailed balance, $(P = P_{\text{trial}} * P_{\text{accept}})$

$$e^{-S(\phi)} P(\phi \to \phi') = e^{-S(\phi')} P(\phi' \to \phi), \tag{2.21}$$

which is a sufficient condition for convergence to the equilibrium distribution.

As new configurations are calculated from previous ones, it is clear that subsequent 'snapshots' of the system are not statistically independent of each other. In order to carry out a correct statistical error analysis it is therefore desirable to step through configuration space rather quickly, minimizing the number of intermediate configurations which have to be discarded because they do not provide information independent of the previous state. The Metropolis algorithm is local and can be implemented efficiently. However, either the new value $\phi'$ is close to the old one, in which case the change in the action is small and its acceptance is likely, or the new $\phi'$ is far from the old one. In the latter case the change in the action is large, however, and the acceptance rate drops exponentially. Both choices result in a slow exploration of configuration space. A somewhat better approach in this respect has therefore been to pick a $\phi'(n)$ not randomly from the whole manifold but with a weighting proportional to the Boltzmann factor (Creutz *et al* 1979, Creutz 1980),

$$dP_{\text{trial}}(\phi') \sim \exp\{-S(\phi')\}\,d\phi', \tag{2.22}$$

i.e. the field $\phi(n)$ is equilibrated in the local heat-bath provided by its neighbours. In this case the change is always accepted. The integration over the group, which is needed in order to select the new field $\phi'$ according to the correct distribution given by (2.22), may, however, be difficult to implement efficiently†, in particular for $SU(N)$ gauge theories with $N \geqslant 3$. For those, one has devised a so-called pseudo-heat bath (Cabibbo and Marinari 1982) in which a new $SU(3)$ matrix is obtained from the old one by constructing $U' = a_2 a_1 U$, where the $a_i$ belong to 2 different $SU(2)$ subgroups of $SU(3)$ and are subsequently generated according to (2.22).

*2.2.2. Critical slowing down: overrelaxed algorithms.* It has been mentioned already in the previous paragraph that subsequent configurations in the Markov chain are not necessarily independent of each other. The number of steps in the Markov chain over which such a correlation extends is quantified by the autocorrelation time $\tau_{\text{exp}}$,

$$C_{\mathcal{O}}(\tau) = \langle \mathcal{O}(t+\tau)\,\mathcal{O}(t)\rangle \sim e^{-\tau/\tau_{\text{exp}}}. \tag{2.23}$$

In principle, the autocorrelation time depends on the observable $\mathcal{O}$. However, with $\tau_{\text{exp}}$, usually the relaxation time of the slowest mode is meant. One can also define an integrated autocorrelation time $\tau_{\text{int},\mathcal{O}} = \frac{1}{2}\int d\tau C_{\mathcal{O}}(\tau)/C_{\mathcal{O}}(0)$, which needs not to be the same as $\tau_{\text{exp}}$ and typically turns out to be somewhat smaller than $\tau_{\text{exp}}$. If the number of generated configurations is $M$ than only $M/\tau_{\text{int},\mathcal{O}}$ statistically independent measurements of $\mathcal{O}$ can be performed. Close to a critical point, i.e. when the continuum limit is approached and a (dimensionless) correlation length $\xi_L$ diverges, the autocorrelation time also diverges. Both are related through a scaling law

$$\tau_{\text{exp}} \sim \xi_L^z, \tag{2.24}$$

where $z$ denotes a dynamic critical exponent. The divergence of $\tau_{\text{exp}}$ near the continuum limit is called critical slowing down. Physically a correlation length $\xi_L$ means that a modification of e.g. a spin at site $n$ influences the orientation of spins being a distance $\xi_L$ apart. A given numerical update scheme, however, requires of the order of $\tau_{\text{exp}}$ updates to communicate changes made at site $n$ over a distance $\xi_L$. Thus only after $\tau_{\text{exp}}$ updates does one obtain a configuration which contains new information, i.e. may be considered as independent. Local algorithms such as the standard Metropolis as well as the heat-bath updating proceed through configuration space like random walks. Correspondingly, their critical exponent has been determined as $z \simeq 2$. An ideal algorithm, on the other hand, would lead to $z = 0$. Much research is therefore going into developing improved methods to reduce this critical slowing down.

A by now widely used algorithm for non-abelian gauge theories is able to reduce the critical exponent to $z = 1$. It is based on the transfer of overrelaxation techniques, as used in solving linear equations, to the Markov process (Adler 1981). Consider (Brown and Woch 1987, Creutz 1987) a single link $U$ in $SU(2)$ gauge theory. The part of the action which depends on $U$ is given by

† It is perhaps worth noting that the efficiency of an algorithm is not independent of the architecture of the computer it is implemented on. Up to now, the fastest computers have been vector machines so that vectorizability is a prerequisite of a fast algorithm. With the availability of powerful parallel machines this might change in the future.

$$S = -\mathrm{tr}\{UV\} + \text{terms independent of } U \tag{2.25}$$

where $V$ denotes the sum of 'staples' around the specified $U$. Let $U_0$ be the value of $U$ which minimizes the action (2.25). Now construct a new link $U'$ by

$$U' = U_0 U^{-1} U_0. \tag{2.26}$$

Then $P_{\text{trial}}(U \to U') = P_{\text{trial}}(U' \to U)$, so that detailed balance is satisfied if the new link is accepted with the usual probability, (2.20). For $SU(2)$, the sum of staples is proportional to an $SU(2)$ matrix again, and $U_0$, as obtained from $U_0 = (1/\det V)V^{-1}$, indeed minimizes $S$, (2.25). Moreover, $\mathrm{tr}\{U'U_0^{-1}\} = \mathrm{tr}\{UU_0^{-1}\}$ so that the action is preserved under the change and the new link is accepted with probability 1. Rewriting (2.26) in the form

$$e^{iu'\sigma} = e^{iu_0\sigma} e^{2iu\sigma} e^{iu_0\sigma} \tag{2.27}$$

shows that the new link lies 'on the opposite side' of $U$ with respect to $U_0$, i.e. at the maximal distance from $U$. Compared to linear equation solvers this amounts to choosing the overrelaxation parameter equal to 2. As the given prescription is action conserving, one has to add standard Metropolis or heat-bath updates to assure ergodicity. For $SU(3)$, the sums of staples are not multiples of an $SU(3)$ matrix and the action is not preserved. One has to perform the accept/reject decision, (2.20), and also provide some method to find the minimum of the action, $U_0$.

Loosely speaking, the reduction of $z$ to $z \simeq 1$ is gained by the right balance between deterministic and ergodic steps. Further improvements seem to require knowledge about the long-distance, slowly moving modes in order to update the corresponding local fields collectively. For Ising systems and other models with global symmetry, where an embedding of Ising spins into the original theory is possible, so-called cluster algorithms have been devised, which are able to obtain $z \simeq 0$ (Swendsen and Wang 1987, Wolff 1989, Hasenbusch 1990). For gauge theories, the local gauge invariance poses a considerable complication. Moreover, it was shown that for theories with field variables which take values in other manifolds than spheres an embedding of Ising-like systems is not possible (Caracciolo *et al* 1992). One therefore has to search for other collective-mode algorithms.

*2.2.3. Fermion simulations: hybrid Monte Carlo algorithm.* The existence of fermions in nature presents an additional complication in numerical lattice calculations. Fermions follow the Pauli exclusion principle and obey anti-commutation relations. These would be comprehensible to a computer only through matrix representations, an approach which is prohibitively memory consuming. As the fermion part of the path integral is Gaussian,

$$S_F = \bar{\psi}(D + m)\psi \tag{2.28}$$

with $D$ being the Dirac matrix and $m$ the fermion mass, one can integrate over the fermion fields analytically,

$$\int \mathscr{D}\psi \mathscr{D}\bar{\psi} \exp(-\bar{\psi}(D + m)\psi) = \det\{D + m\}. \tag{2.29}$$

This manipulation leads to the famous fermion determinant, whose calculation except for small lattices is practically impossible because the number of operations required grows like (volume)$^3$ and suffers from numerical instabilities. However, there are ways to deal with it in

the form of trading the determinant for the inverse of the Dirac matrix. This will be explained in some detail below. Even then, the numerical effort is quite large so that many lattice investigations have been using the so-called quenched approximation. This approximation amounts to setting the determinant equal to 1. Seemingly a crude approximation, a quick calculation reveals that $\det\{D+m\} \stackrel{!}{=} 1$ amounts to neglecting virtual fermion loops,

$$\mathrm{tr}\log\{D+m\} \sim \sum_{k=0}^{\infty} (\frac{1}{m})^{2k} D^{2k} \stackrel{!}{=} 0. \tag{2.30}$$

The Dirac matrix $D$ connects neighbouring lattice sites via a gauge link and contributes only with even powers to the expansion, (2.30), because otherwise the integral over the gauge fields vanishes. For the same reason, only closed loops do not average to zero. Thus, the quenched approximation neglects (virtual) quark loops and treats fermions as static degrees of freedom. Properties of the theory which depend crucially on the fermion dynamics are thus not accessible by studies in the quenched approximation. On the other hand, basic properties of e.g. QCD which are dominated by the non-abelian gluon dynamics should and do survive the approximation. Thus, quenched studies may serve as important guides for many non-perturbative aspects of the theory. Of course, the results have to be checked by calculations in the full theory.

All fermion algorithms in use, which try to take into account the dynamical effects of fermions in the generation of field configurations, re-express the determinant by a path integral over pseudofermion fields i.e. bosonic fields which interact via the fermion matrix (Petcher and Weingarten 1981, see also Fucito *et al* 1981). As the fermion matrix is not positive definite, one first has to square the determinant in order to obtain a regular Boltzmann weight factor,

$$\begin{aligned} \det{}^2\{D+m\} &= \det\{(D+m)\dagger(D+m)\} \\ &= \int \mathscr{D}\phi\,\mathscr{D}\phi^* \exp(\phi^*[(D+m)\dagger(D+m)]^{-1}\phi). \end{aligned} \tag{2.31}$$

Thus one has traded the determinant for the inverse matrix at the cost of simulating twice the number of fermion species. However, in terms of pseudofermionic variables, the fermions can now be dealt with in an ordinary Monte Carlo. Because of the non-locality of the inverse Dirac matrix, any local updating scheme for the gauge fields would though require to recalculate the inverse after each local change in the $U$s. Alternatively, one could change a whole gauge field configuration at once and then recalculate the inverse. However, with ordinary, local updating procedures, the acceptance probability of a global change would drop to zero very quickly with the lattice size.

The hybrid Monte Carlo algorithm (Duane *et al* 1987), which to date is the only algorithm which is exact and also not prohibitively time consuming (at least on lattices which are not enormously large), solves this problem by deliberately preparing a new configuration for a global accept/reject decision. This preparation is based on elements taken from previously developed approximate algorithms. Suppose one adds a quadratic term to the action,

$$\begin{aligned} \mathscr{H} &= \frac{1}{2} \sum_{n,\mu} \mathrm{tr}\,\pi_\mu^2(n) + S_E \\ &= \frac{1}{2} \sum_{n,\mu} \mathrm{tr}\,\pi_\mu^2(n) + S_G(U) + \phi^*[(D+m)\dagger(D+m)]^{-1}\phi. \end{aligned} \tag{2.32}$$

The extra term can be integrated out analytically and does not change vacuum expectation values. This expression, (2.32), is now taken as a Hamiltonian from which equations of motion in a fictitious time $\tau$ are derived. The $\pi$ fields can be considered as conjugate momenta to the fields $U$, slightly modified to preserve the gauge fields as elements of the gauge group,

$$\dot{U}_\mu(n) = i\pi_\mu(n)U_\mu(n). \tag{2.33}$$

With the pseudofermion fields $\phi$ kept constant during the evolution in the time $\tau$ (Gottlieb *et al.* 1987a), the second set of Hamiltonian equations is given by

$$i\dot{\pi}_\mu(n) = \left[U_\mu(n)\frac{\partial}{\partial U_\mu(n)}\{S_G(U) + \phi^\dagger[(D+m)^\dagger(D+m)]^{-1}\phi\}\right]_{TA} \tag{2.34}$$

where the subscript $TA$ denotes the traceless anti-Hermitian part in colour space, $A_{TA} = (A - A^\dagger) - (1/N)\,\mathrm{tr}\,(A - A^\dagger)$. This step is, of course, the time consuming one as it requires to calculate the inverse of the fermion matrix. With momenta conjugate to the pseudofermion fields added, a pure Hamiltonian evolution has been used in the past for simulations of the full theory (Callaway and Rahman 1982), exploiting the fact that for large systems the canonical distribution, $\exp(-\mathscr{H})$ is very sharply peaked around the microcanonical one, $\delta(E - \mathscr{H})$. The advantage of the Hamiltonian evolution is its relatively fast progressing through phase space. However, there are reasons to believe that it violates ergodicity. Alternatively, Langevin methods (Parisi and Wu 1981, Fukugita and Ukawa 1985, Batrouni *et al* 1985) have been used, which replace the two first order differential equations given above, i.e. a second order derivative in the fields, by a single first order one. Generically, the Langevin evolution is given by

$$\dot{\phi} = -\frac{\partial}{\partial\phi}S + \eta \tag{2.35}$$

which also includes a noise term $\eta$ to guarantee ergodicity. However, a pure Langevin evolution is basically a random walk through phase space and thus progress is rather slow.

In the hybrid Monte Carlo algorithm the system is guided through phase space by combining Langevin steps with molecular dynamics iterations. Thereby the advantages of both, Lanvevin and microcanonical algorithm, fast progress through phase space and ergodicity, are utilized. To be specific, at the beginning of a so-called trajectory, the momenta as well as the pseudofermion fields are refreshed in random manner, for QCD (Gottlieb *et al* 1987a),

$$\begin{aligned}\pi_\mu(n) &= \sum_{a=1}^{8}\lambda_a r_\mu^a(n)\\ \phi^i(n) &= \sum_m\sum_{j=1}^{3}(D+m)^\dagger_{ij}(n;m)r^j(m).\end{aligned} \tag{2.36}$$

Here, the $r$'s represent (two different) sets of Gaussian random numbers with variance $\langle r^2\rangle = \frac{1}{2}$ the $\lambda$'s are the generators of the gauge group and $a$ and $i, j$ are colour indices. Note in passing that this gives the desired distributions of the $\pi$ and $\phi$ fields. This step is then followed by a number $N_{MD}$ of molecular dynamics iterations, (2.33) and (2.34). At the end of such a

trajectory one has deliberately prepared a configuration which then is accepted as new configuration with probability

$$P_{\text{accept}} = \min\{1, \exp(-[\mathcal{H}_{\text{final}} - \mathcal{H}_{\text{initial}}])\}. \tag{2.37}$$

If the integration of the equations of motions could be carried out exactly, the acceptance probability for a configuration at the end of a trajectory would be unity because energy is preserved in Hamiltonian dynamics. However, the necessity to solve the equations of motion numerically, i.e. the introduction of finite time step sizes $d\tau$, needed to discretize the $\tau$ derivatives in (2.33)–(2.34), unavoidably introduces integration errors which lead to slight violations of energy conservation. These errors can be studied by means of the Fokker–Planck equation (Batrouni *et al* 1985). It turns out that they can partially be absorbed into a renormalization of the coupling constants. But there are also non-integrable terms. The hybrid Monte Carlo compensates for these errors by performing the above global accept/reject decision about the accumulated changes of the configuration at the end of a trajectory (Scalettar *et al* 1986, Duane *et al* 1987). This Monte Carlo element makes the algorithm an exact one. The evolution along a trajectory is taken only as a way to very carefully prepare a new tentative update of the system as a whole.

In order to be a viable Monte Carlo procedure, the hybrid Monte Carlo algorithm has to maintain detailed balance. This is achieved by letting the fields and their conjugate momenta evolve according to a leapfrog discretization scheme. In its simplest version this is given by

$$\begin{aligned} \pi(\tau + d\tau) &= \pi(\tau) + \dot{\pi}(\tau + \frac{1}{2}d\tau)d\tau + O(d\tau^3), \\ U(\tau + \frac{1}{2}d\tau) &= e^{i\pi(\tau)d\tau}U(\tau - \frac{1}{2}d\tau) + O(d\tau^3). \end{aligned} \tag{2.38}$$

As indicated, the errors are proportional to $d\tau^3$ while in the initial and final half steps of the $U$ field evolution the error is $O(d\tau^2)$. In the end, this amounts to an energy violation $\sim V d\tau^4$, where $V$ is the 4-dimensional lattice volume (Creutz 1988, Gupta R *et al* 1988b, Horsley *et al* 1989, Gupta S *et al* 1990). Thus the time step size has to be scaled as $V^{-1/4}$ in order to maintain a constant acceptance probability. Of course, this error can be reduced by decreasing the time step size appropriately but then progress through phase may become slow. Therefore, it is worthwhile to think about refinements of the leapfrog scheme, (2.38), (Campostrini and Rossi 1990, Sexton and Weingarten 1992). Another important issue concerns the critical behaviour of the hybrid Monte Carlo. Studies of simpler models like the 2D $XY$ model suggest a dynamic critical exponent of $z \simeq 1$, if the trajectory length is varied proportionally to the correlation length, $\tau = N_{MD}\delta\tau \sim \xi_L$, and $z \simeq 2$ for fixed $\tau$ (Kennedy and Pendleton 1990, Gupta S 1992a).

In simulations with dynamical fermions, by far the largest fraction of computing time goes into repeatedly calculating the inverse of the Dirac matrix. For that purpose, iterative inversion solvers like the conjugate gradient for staggered and the minimal residual algorithm for Wilson fermions are used. These schemes already exploit the sparse nature of the Dirac matrix rather efficiently. Still, the number of iterations necessary to reach a certain accuracy depends on the fermion mass via the condition number

$$N_{\text{iter}} \sim \frac{|\lambda|_{\max} + m}{|\lambda|_{\min} + m} \sim \frac{1}{m}, \tag{2.39}$$

where $\lambda$ denotes an eigenvalue of the Dirac matrix. This explains the high cost of

simulations with small fermion masses. Therefore, the investigation of preconditioning techniques like e.g. ILU decomposition, of convergence accelerators as e.g. Fourier acceleration or of multigrid methods is a very active area of research at present (see for instance Herrmann and Karsch 1991, Kalkreuter 1992).

### *2.3. Continuum limit and critical phenomena*

A central question to be answered in any lattice study is in how far results are influenced by the lattice discretization or directly represent continuum physics. Clearly on a coarse lattice with large lattice spacings rotational symmetry is violated and calculations of, for instance, correlation functions, will be affected by this. However, these lattice artefacts should vanish in the continuum limit.

Physical quantities are calculated on the lattice in units of the lattice spacing $a$; for instance, a mass or inverse correlation length will be given in units of $a^{-1}$, the string tension in units of $a^{-2}$ and the energy density in units of $a^{-4}$. The continuum limit, $a \to 0$, should be taken while keeping physical quantities like the correlation length, $\xi \sim 1/m_{\text{Hadron}}$, fixed. On the lattice the continuum limit thus corresponds to a point in parameter space where the lattice correlation length, $\xi_L = \xi/a$, diverges. The continuum limit has to be taken at the critical point of the statistical model defined by the lattice partition function (2.8). In fact, it is a central task of lattice calculations to identify the critical points in parameter space at which a continuum theory can be defined. *A priori* it is not insured that the QFT defined at such a point coincides with the perturbatively studied continuum theory. The $SU(2)$-Higgs model as well as the $U(1)$ gauge theory with fermions on the lattice provide examples where the known fixed points may lead to trivial non-interacting theories. We will discuss these models further in section 5. Here we will concentrate on a discussion of the continuum limit of QCD.

In the case of 4-dimensional QCD with massless quarks, the lattice action itself does not contain any dimensional parameter. The lattice cut-off $a^{-1}$ enters through the renormalization of the bare couplings, i.e. the gauge coupling $g^2$ and the quark masses $m_i$. It is generally expected that the continuum limit of lattice QCD is reached in the limit $g^2 \to 0$, where the relation between $g^2$ and $a$ is known from a perturbative analysis of the renormalization group equation. To two-loop order one finds for $n_f$ massless fermion flavours and colour gauge group $SU(N)$,

$$a\Lambda_L = (b_0 g^2)^{-b_1/2b_0^2} e^{-1/2b_0 g^2} \tag{2.40}$$

with $b_0$, $b_1$ given by

$$\begin{aligned} b_0 &= \frac{1}{16\pi^2}\left[\,11\frac{N}{3} - \frac{2}{3}n_f\right] \\ b_1 &= \left(\frac{1}{16\pi^2}\right)^2\left[\frac{34}{3}N^2 - \left(\frac{10}{3}N + \frac{N^2-1}{N}\right)n_f\right]. \end{aligned} \tag{2.41}$$

Here $\Lambda_L$ is an unknown scale parameter, not fixed by the theory. The above relation can then be used to eliminate the cut-off from calculated, dimensionless quantities ($m_{\text{Hadron}}$, $\sqrt{\sigma}a$) in favour of the scale parameter $\Lambda_L$. If the lattice simulations have been performed in the continuum regime, results should be cut-off independent, i.e. physical quantities expressed in units of $\Lambda_L$, like $m_{\text{Hadron}}/\Lambda_L$ or $\sqrt{\sigma}/\Lambda_L$, should be independent of the coupling $g^2$ used in the actual calculation. Numerical studies of the QCD β-function using Monte Carlo

renormalization group techniques gave evidence that the asymptotic scaling behaviour, described by (2.40), is approximately valid for $g^2 < 1$ (Bowler *et al* 1986, Gupta R *et al* 1988a). For $g^2 \geqslant 1$, however, strong violations of asymptotic scaling have been found. In fact, these violations also gave rise to the speculation that the continuum limit of lattice QCD will not be reached at $g^2 = 0$, but may have to be taken at finite $g^2$ (Patrascioiu and Seiler 1992). The Monte Carlo data we are going to discuss in the following certainly cannot rule out such a possibility as they can probe only a finite interval of $g^2$ values. However, they also do not show any evidence for such an unconventional behaviour.

Detailed studies of the scaling and asymptotic scaling behaviour have been performed recently in pure $SU(N)$ gauge theories. The simplest physical quantities accessible in this case are the string tension, $\sigma$, as well as the deconfinement transition temperature, $T_c$. Both quantities have been studied on large lattices over a relatively wide range of couplings, which, nonetheless, does not allow to go to very small values of $g^2$. It turns out that the ratio of these observables, $T_c/\sqrt{\sigma}$, indeed to a large extent is insensitive to variations of the cut-off. This is shown in figure 1 for the $SU(2)$ and $SU(3)$ gauge theory.

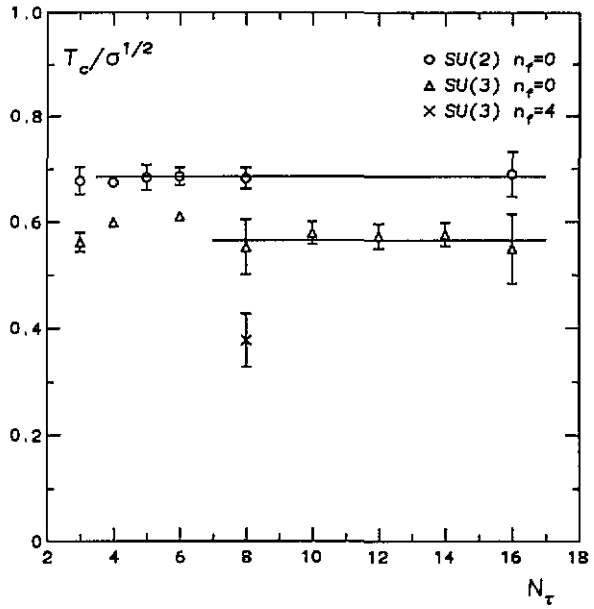


**Figure 1.** $T_c/\sqrt{\sigma}$ for $SU(2)$ (circles) and $SU(3)$ (triangles) pure gauge theory as well as 4-flavour QCD (cross).

Averaging over the ratios measured for small values of $aT_c$ one finds

$$\frac{T_c}{\sqrt{\sigma}} = \begin{cases} 0.69 \pm 0.02 & SU(2) \\ 0.56 \pm 0.03 & SU(3) \end{cases} . \tag{2.42}$$

It is rather remarkable that scaling of $T_c/\sqrt{\sigma}$ is valid in the case of $SU(2)$ to a high degree over the entire range of lattice spacings from $aT_c \simeq 0.25$ on downwards. Using as an input the experimental value for the string tension, $\sqrt{\sigma} = (420 \pm 20)\,\mathrm{MeV}$, this corresponds to lattice spacings $a \lesssim 0.5\,\mathrm{fm}$, i.e. only little less than typical hadronic scales of 1 fm. For $SU(3)$

**Table 1.** The ratio of various physical observables. The hadron masses have been taken from (Billoire *et al* 1985, Langhammer 1986) ($SU(2)$, $n_f = 0$), (Kogut *et al* 1991) ($SU(2)$, $n_f = 4$), (Cabasino *et al* 1991, Gupta R *et al* 1991a) ($SU(3)$, $n_f = 0$) and (Altmeyer *et al* 1993) ($SU(3)$, $n_f = 4$). Results for $n_f = 2$ have been taken from (Gottlieb *et al* 1987b). With $m_G$ we denote the mass of the lowest lying glueball state, $0^{++}$.

| | $T_c/\sqrt{\sigma}$ | $T_c/m_\rho$ | $T_c/m_N$ | $\sqrt{\sigma}/m_\rho$ | $m_G/m_\rho$ |
|---|---|---|---|---|---|
| $SU(2)$ | | | | | |
| $n_f = 0$ | 0.69(2) | 0.25(3) | — | 0.36(3) | 1.4(3) |
| $n_f = 4$ | 0.38(2) | 0.15(3) | — | 0.39(3) | 1.1(2) |
| $SU(3)$ | | | | | |
| $n_f = 0$ | 0.57(3) | 0.31(3) | 0.24(3) | 0.53(9) | 1.8(3) |
| $n_f = 2$ | — | 0.19(1) | 0.12(1) | — | — |
| $n_f = 4$ | 0.38(5) | 0.17(1) | 0.11(1) | 0.45(6) | — |

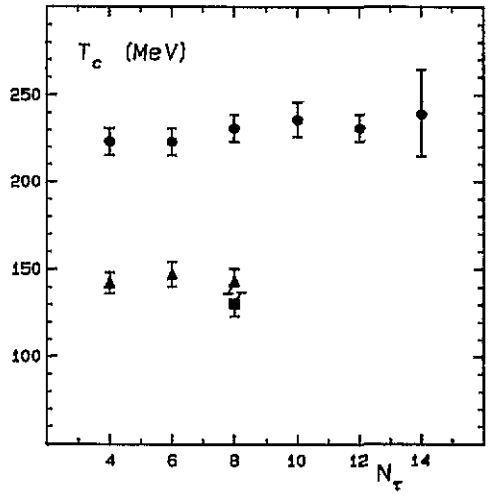


**Figure 2.** $T_c$ in MeV extracted from $m_\rho$ for QCD with $n_f = 0$ (dots), 2 (triangles) and 4 (square) flavours of light quarks.

the same seems to hold for $a \lesssim 0.25$ fm. A similar behaviour is found in the ratio $T_c/m_\rho$, shown in figure 2. Here we have also included results from simulations with two light quark flavours ($n_f = 2$) (Gottlieb *et al* 1987b, Bernard *et al* 1992d, Gottlieb *et al* 1992). Results for various ratios of physical observables are summarized in table 1.

Despite this impressive scaling behaviour, the lattice simulations clearly have not been performed in the asymptotic scaling regime defined as the regime of validity of (2.40). This becomes obvious from the behaviour of $T_c/\Lambda_{\overline{MS}}$ shown in figure 3†. The scaling behaviour found for various ratios of physical observables suggests, however, that the violations of asymptotic scaling found in individual quantities are of common origin and could be

† We use the more familiar continuum scale parameter $\Lambda_{\overline{MS}}$ rather than the lattice scale parameter $\Lambda_L$. Both are related through $\Lambda_L/\Lambda_{\overline{MS}}^{N_{af}} = \exp\{(1/2b_0)[(1/8N) - 0.169956N + P_4 n_f]\}$, where $P_4 = 0.002\,6248$ for staggered fermions and $P_4 = 0.006\,8870$ for Wilson fermions (Weisz 1981, Sharatchandra *et al* 1981).

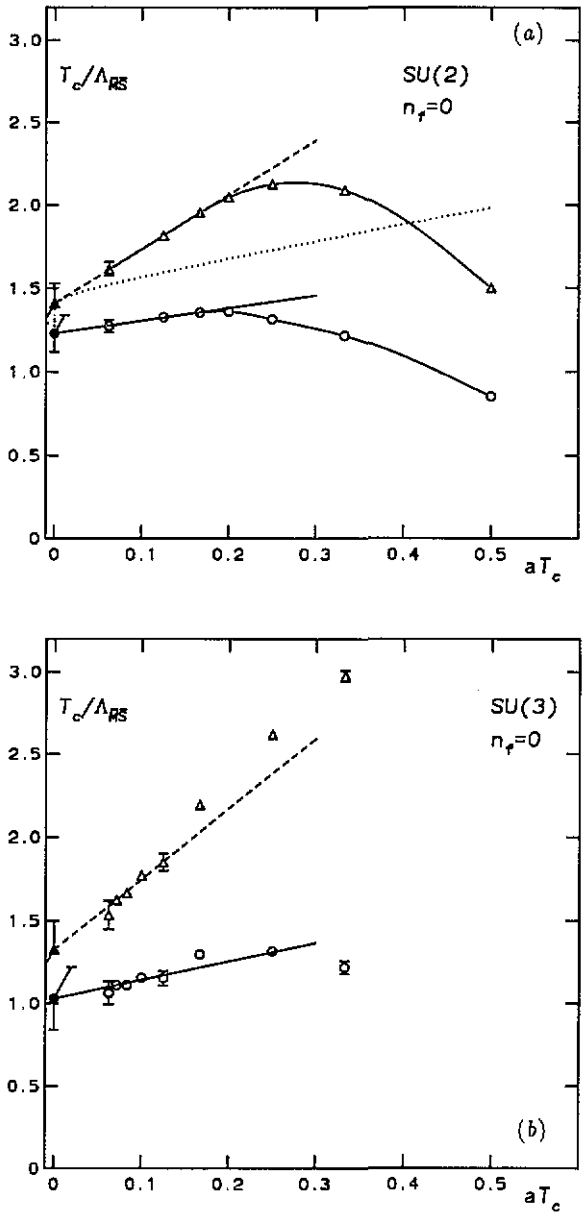


**Figure 3.** $T_c/\Lambda_{\overline{MS}}$ (*a*) and $\sqrt{\sigma}/\Lambda_{\overline{MS}}$ (*b*) for the $SU(3)$ pure gauge theory obtained by using (2.40) with the bare coupling, $\beta$ (triangles), and the effective coupling $\beta_E$ (circles).

removed in a suitable renormalization scheme. There have been various suggestions for the choice of renormalized couplings, which could improve the asymptotic scaling behaviour (Parisi 1980). In figure 3 we also show $T_c/\Lambda_{\overline{MS}}^{N,0}$ obtained from (2.40) after replacing the bare coupling $\beta$ by

$$\beta_E = \frac{N^2 - 1}{4\langle P \rangle}, \tag{2.43}$$

where $\langle P \rangle$ denotes the expectation value of the Euclidean action density given by the plaquette term defined in (2.12).

The rather weak dependence of physical quantities on the coupling in the renormalized, $\beta_E$-scheme allows us to use physical quantities, known from experiment, as input and determine the unknown QCD scale parameter. From figure 3 we deduce for the $SU(3)$ gauge theory $\Lambda_{\overline{MS}}^{3,0} = (240 \pm 30)$ MeV using the string tension value $\sqrt{\sigma} = (420 \pm 20)$ MeV as input. Similar results have been obtained from studies of the short distance part of the heavy quark potential (Bali and Schilling 1993, Booth *et al* 1992) and the 1P–1S fine splitting in the charmonium spectrum (El-Khadra *et al* 1992), which led to consistent values for $\Lambda_{\overline{MS}}^{3,0}$. Also in the case of $SU(2)$ gauge theory the values obtained for $\Lambda_{\overline{MS}}^{2,0}$ are consistent with the above value (Fingberg *et al* 1993, Michael 1993, Lüscher *et al* 1993). We note, however, that the physics of the $SU(2)$ gauge theory clearly is different from that of the $SU(3)$ gauge theory. This is particularly evident from the ratio $\sqrt{\sigma}/m_\rho$, which can be obtained from table 1,

$$\frac{\sqrt{\sigma}}{m_\rho} = \begin{cases} 0.36 \pm 0.04 & SU(2) \\ 0.54 \pm 0.05 & SU(3) \end{cases}. \tag{2.44}$$

This should be compared with the experimental value, $\sqrt{\sigma}/m_\rho = 0.545 \pm 0.026$. Thus quenched QCD (pure $SU(3)$ gauge theory) provides a surprisingly good approximation to the real world in this case. On the other hand, a strong dependence of $\Lambda_{\overline{MS}}^{3,n_f}$ on the number of flavours is known from perturbative analysis of high energy data. The calculation of the string tension for four flavour QCD (Born *et al* 1991a) provides indications from the lattice that dynamical quarks reduce the value of $\Lambda_{\overline{MS}}^{3,n_f}$ substantially, leading to $\Lambda_{\overline{MS}}^{3,4} = (150 \pm 40)$ MeV in the $\beta_E$ scheme.

## 3. QCD at low energies

Quantum Chromo Dynamics is generally accepted as the microscopic theory of the strong interactions. At large momentum transfers, due to asymptotic freedom, QCD has been exploited perturbatively with great success. At low energies, however, the effective quark–gluon coupling becomes large and non-perturbative techniques have to be adopted. Numerical lattice investigations provide a unique possibility to study the long-range properties of QCD with, in principle, no approximation. The aim of lattice QCD is to collect convincing evidence for anticipated basic features of QCD at large distances, in particular for confinement and spontaneous chiral symmetry breaking. Moreover, it is attempted to verify phenomenological concepts and to predict parameters for experiment and model building which are inaccessible otherwise. Naturally, one has to calibrate the precision of lattice investigations by confronting lattice results with experimental data.

### *3.1. Confinement and the heavy quark potential*

Charmonium and in particular bottonium systems are sufficiently heavy to allow non-relativistic concepts to be adopted. The interactions between these heavy quarks can then be described by means of a potential. Also the confinement hypothesis of QCD can be expressed in a simple way namely in terms of a potential which grows when the distance between heavy quarks is increased.

Phenomenologically, the potential is decomposed into a spin-independent part which is responsible for confinement, and fine-structure corrections which involve spin–orbit and spin–spin interactions. The spin-independent part $V_C(R)$ of the potential is empirically rather well described by a superposition of a term which rises linearly with distance and leads to the confinement of quarks, plus a Coulomb-like correction which is motivated by one-gluon exchange dominating at small distances. The prototype of these potential ansätze is given by the Cornell potential (Eichten *et al* 1975),

$$V_C(R) = -\frac{4}{3}\frac{\alpha}{R} + \sigma R, \tag{3.1}$$

with a fixed Coulomb coefficient $\alpha$ and $\sigma$ being the string tension, $\sqrt{\sigma} \simeq 420\,\mathrm{MeV}$. Modifications include a perturbatively running Coulomb coefficient $\alpha(R)$ at small $R$ and various interpolation prescriptions between the small and large distance behaviour (for an overview see e.g. Kühn and Zerwas 1988). In the distance range probed by charmonium and bottonium states the various ansätze are in numerical agreement. The differences show up in the short distance properties. This region will be probed by toponium, if the top quark is not too heavy. At present, quantities which depend on wave functions at the origin like e.g. leptonic widths favor a logarithmically softened Coulomb singularity as in QCD-like potentials (Buchmüller and Cooper 1988).

The potential is obtained in a gauge-invariant way from the Wilson loop (Wilson 1974),

$$W(R,T) = \langle \exp(\mathrm{i}\oint_{R\times T} \mathrm{d}x_\mu A_\mu)\rangle \sim \exp(-V_C(R)T), \tag{3.2}$$

which describes the propagation of a static quark–antiquark pair, separated by a distance $R$, in Euclidean time $T$. In (3.2) it has been assumed that $T$ is sufficiently large so that the ground state potential $V_C$ dominates the expectation value and excitations of the string of colour fields between the heavy quarks are exponentially suppressed.

The confinement potential has been the target of quite a few investigations starting with the first numerical lattice studies of Creutz on $5^4$ lattices (Creutz 1980). As a major technical improvement, it was possible to construct operators for the colour string which have an increased overlap with the ground state (Teper 1986, Albanese *et al* 1987). This allows to reliably extract $V_C$ already from Wilson loops with smaller time extent. The results of recent analyses in the quenched approximation (Bali and Schilling 1992, Booth *et al* 1992) on lattices up to size $32^4$ are shown in figure 4. The data reach distances almost up to $R = 2\,\mathrm{fm}$ and demonstrate a linear rise at large separations very nicely. This result as well as observations in earlier attempts represent important support for the confinement hypothesis.

The linear rise at large distances is accompanied by a Coulomb-type behaviour at small $R$. At not too small quark—antiquark separations, the coefficient of the Coulomb term is compatible with a universal strength $\pi/12$ predicted by string models (Lüscher *et al* 1980) for distances $R \geq 0.3\,\mathrm{fm}$ (Alvarez 1981). Below 0.1 to 0.2 fm it is expected that the potential is adequately described by perturbative 1-gluon exchange (Fischler 1977, Billoire 1980),

$$V(R) = -\frac{N^2-1}{2N}\frac{\alpha(R)}{R} \tag{3.3}$$

with

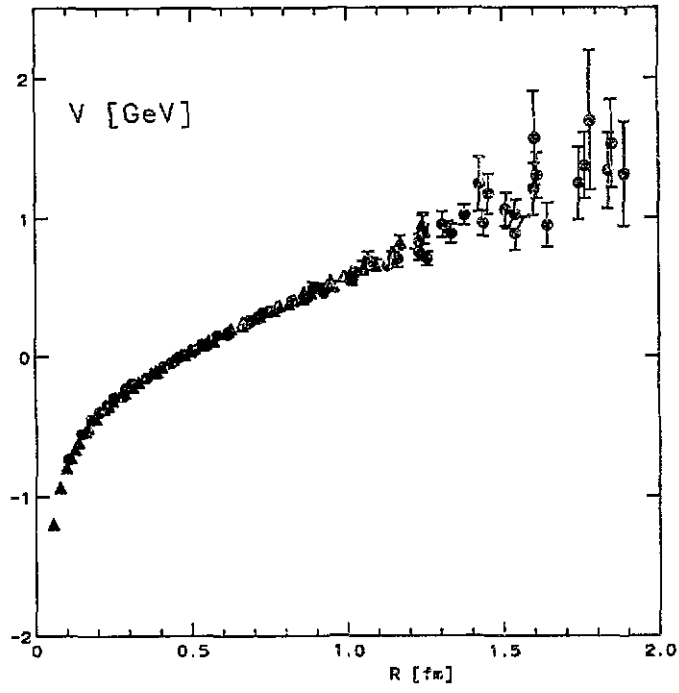


**Figure 4.** The heavy quark potential in quenched QCD (data obtained from Bali and Schilling 1992).

$$\alpha(R) = \frac{4\pi}{b_0 \ln(1/R^2\Lambda^2_{\overline{MS}})}\left[1 - \frac{b_1}{b_0^2}\frac{\ln\ln(1/R^2\Lambda^2_{\overline{MS}})}{\ln(1/R^2\Lambda^2_{\overline{MS}})} + \frac{(31N - 10n_f)/9b_0 + 2\gamma_E}{\ln(1/R^2\Lambda^2_{\overline{MS}})}\right], \quad (3.4)$$

where $b_0$ and $b_1$ are given in (2.41). Indeed, quantitative analyses of the short distance behaviour (Michael 1992, Bali and Schilling 1993, Booth *et al* 1992) do find evidence for a 'running' $\alpha(R)$ in accordance with (3.4). By setting the scale from the string tension, the QCD $\Lambda$ parameter can be extracted from the measured $\alpha(R)$. One finds, in physical units, $\Lambda^{3,0}_{\overline{MS}} = (240 \pm 30)$MeV (for $SU(3)$). This result, obtained from the short distance properties of the theory, compares successfully with the results of other approaches mentioned in section 2.3. Moreover, a similar analysis in quenched $SU(2)$ is in agreement with a program in which long and short distances are covered in a step-wise manner, by working on a variety of different lattices sizes and matching them by means of a variant of the renormalization group procedure (Lüscher *et al* 1993). Thus the originally non-perturbative lattice approach is becoming capable of reaching into the short distance regime where results can be matched directly to perturbative calculations. However, compared to recent LEP data (or to phenomenologically successful potentials) the lattice results for the running coupling constant are too low. One and presumably the main reason for this discrepancy is expected to be the quenched approximation. The coefficient $b_0$ is strongly dependent on the number of flavours $n_f$, leading to a difference of about 30% between $n_f = 0$ and $n_f = 4$. This effect will partially be counteracted by an unknown shift in $\Lambda^{3,n_f}_{\overline{MS}}$. Moreover, the quenched string tension from which usually the scale is taken, is not a physical quantity. Equating it to the

'experimental' value of 420 MeV neglects the effects of quark loops. In particular, the potential in full QCD is expected to flatten out at some distance due to quark pair creation. This could also affect the numerical value of the string tension (see, however, (2.44)).

Results from simulations of full, QCD, i.e. with light dynamical quarks taken into account, are beginning to emerge from rather large lattices. The currently accessible distances are in the range $0.1 \leq R \leq 1.0$ fm so far. For those quark–antiquark separations, investigations in the full theory (Born *et al* 1991a) confirm a Coulomb plus linear form of the potential and thus support standard heavy quarkonium phenomenology. At distances larger than 1 fm one hopes for indications that the flux tube connecting the heavy quarks breaks. This is expected because of the spontaneous creation of light quark–antiquark pairs which screen the colour charges of the heavy quarks.

Fine and hyperfine splittings in quarkonium spectra, beyond their phenomenological importance, are interesting because they depend on the spin-structure of the confining Bethe–Salpeter kernel. They can be derived from the spin-dependent potential, the most general form of which is obtained from a systematic expansion in the inverse quark mass $1/m$ and is given by the Breit–Fermi parameterization,

$$\begin{aligned} V_{\text{spin}}(R) &= \frac{1}{2m^2R}\,\mathbf{LS}(V_0' + 2V_1' + 2V_2') \\ &+ \frac{1}{m^2}\left[\frac{1}{R^2}\,(\mathbf{RS}_1)(\mathbf{RS}_2) - \frac{1}{3}\mathbf{S}_1\mathbf{S}_2\right]V_3 \\ &+ \frac{2}{3m^2}\,\mathbf{S}_1\mathbf{S}_2 V_4 \end{aligned} \tag{3.5}$$

here written for the case of two identical quark masses $m$. The three contributions represent subsequently the spin–orbit, the tensor and the spin–spin parts. The components $V_i$ can be extracted from correlations among the colour-electric and colour-magnetic fields (Eichten and Feinberg 1981) in Wilson loops, $V_{1,2} \sim \langle B_i E_j\rangle_W$ and $V_{3,4} \sim \langle B_i B_j\rangle_W$. $V_1$ and $V_2$ are related to the confinement potential through the Gromes identity (Gromes 1984), $V_2 - V_1 = V_C$, so that $V_1$ and $V_2$ cannot be of short range both at the same time. In fact, if the confining Bethe–Salpeter kernel has a scalar Dirac structure, a long-range component resides in $V_1 \simeq -V_C$ while for vector confinement it resides in $V_2 \simeq V_C$. As a consequence, the long-range part of the spin–orbit potentials is markedly different. Experimentally, the ratios of the $P$-level fine splittings in charm and bottom decays allow one to differentiate between the two cases. They strongly favour scalar confinement while pure vector confinement seems to be ruled out by the data (Buchmüller and Cooper 1988).

The lattice analyses (Campostrini *et al* 1986, Huntley and Michael 1987, Laermann *et al* 1992) conform with this picture very nicely. Figure 5 summarizes the findings of a study in full QCD (Laermann *et al* 1992). While $dV_1/dR$ is flat within the error bars, $dV_2/dR$ and $V_3$ drop rapidly and appear to be well described by perturbative one-gluon exchange. The spin–spin term is practically zero for $R \geq \sqrt{2}a$, which is compatible with the perturbative behaviour $V_4(R) \sim \delta(R)$.

### *3.2. Chiral symmetry*

The spectrum of QCD and many transition amplitudes of light quark states reveal the characteristic pattern of a theory whose chiral symmetry is spontaneously broken. For zero-

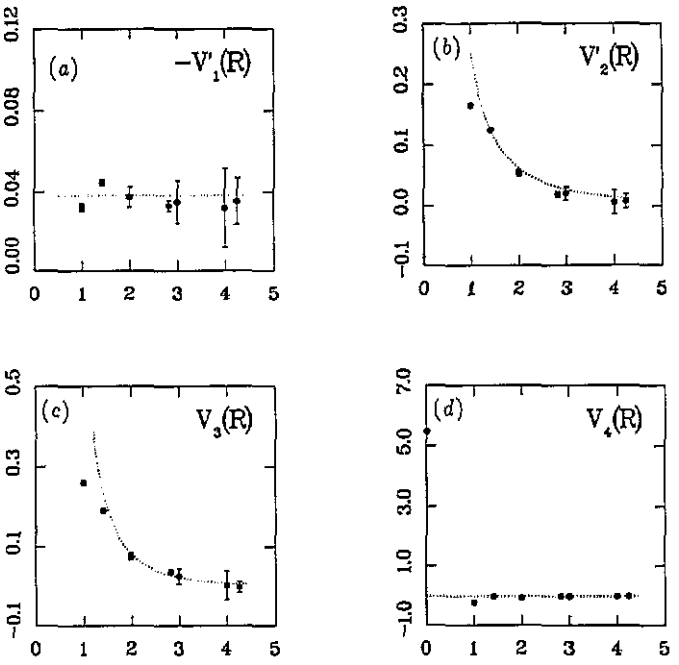


**Figure 5.** The spin dependent potentials in full QCD, taken from (Laermann *et al* 1992). The results were obtained with a quark mass of $m_q \simeq 35$ MeV. The dotted lines, except for $V'_1(R)$, indicate the perturbative prediction of a short-ranged vector potential.

mass quarks the action is invariant under separate transformations of left-handed and right-handed quarks. However, this global chiral symmetry is not observed in the hadron spectrum. Instead one finds the typical features of spontaneous symmetry breaking: a pion whose mass is nearly zero on a typical hadronic scale, $m_\pi^2/m_\rho^2 = 0.04$, which thus might be interpreted as the Goldstone boson of the broken symmetry, as well as a non-vanishing value for the quark condensate in the vacuum. Both features are clearly of non-perturbative nature and invite a first principle lattice investigation.

The result of a recent investigation of these questions in full QCD with staggered fermions (Altmeyer *et al* 1993) is shown in figure 6. At vanishing quark mass the numerical

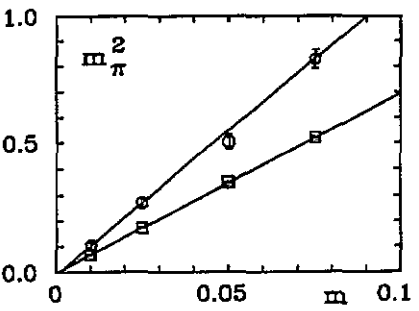


**Figure 6.** The pion mass squared as a function of the quark mass $m$ (boxes). The second data set (circles) are the results for one of the additional pseudo scalar mesons in the staggered fermion discretization which also become Goldstone bosons in the continuum limit.

algorithms to invert the Dirac matrix

$$\langle\bar{\psi}\psi\rangle = \mathrm{tr}(D+m)^{-1}, \tag{3.6}$$

do not work. One thus has to calculate at finite quark mass and then to extrapolate to the chiral limit. From chiral perturbation theory (Gasser and Leutwyler 1982), it is expected that the pion mass squared is linear in the quark mass. Indeed, the lattice data for the pion mass, shown in figure 6, follow a linear quark mass dependence rather nicely. Moreover, in the chiral limit, at zero quark mass, the pion mass vanishes. Furthermore, the quark condensate has a finite intercept at zero quark mass. The numerical value of the renormalization group invariant condensate for one flavour is obtained as $\langle\bar{u}u\rangle^{RGI} \simeq (200\,\mathrm{MeV})^3$ with a 10% error, quite close to the $(190\,\mathrm{MeV})^3$ extracted by means of current algebra techniques from low-energy pion reactions. Moreover, one can calculate the pion decay constant $f_\pi$ from the appropriate matrix element and exploit the Gell Mann–Oakes–Renner formula, $f_\pi^2 m_\pi^2 = m\langle\bar{u}u + \bar{d}d\rangle$, in the limit of vanishing quark mass in order to check this value. Within 10 to 20% error agreement has been found.

### *3.3. Meson and baryon spectroscopy*

A central problem of QCD at low momentum is the computation of the hadron spectrum. As most of the low-lying hadron masses are known from experiment very precisely, this branch of lattice calculations may have limited predictive power as far as purely numbers are concerned. Nevertheless, these calculations are important to verify that the non-perturbative dynamics of QCD at low energies explains the experimental spectrum and to control the degree of accuracy reached in a numerical investigation.

The masses of hadrons are obtained from investigating the propagation of hadrons in (Euclidean) time, $\langle H(t)|H^\dagger(0)\rangle$. By inserting a complete set of energy states and projecting to zero momentum, one can extract the mass of the lightest hadron with the right quantum numbers from the exponential decay at large times

$$\langle H(t)|H^\dagger(0)\rangle \to \mathrm{e}^{-m_H t}. \tag{3.7}$$

Generally, the operators $H$ are sensitive to all hadrons with a given set of quantum numbers specified by $H$. The matrix element, (3.7), thus contains contaminations of excited states so that a large time extent is required in order not to overestimate the mass of the lightest hadron. Alternatively, one tries to construct operators with a large projection onto the ground state hadron. These are typically extended operators which approximate an anticipated S-wave like shape of the wave function.

A quantity that is very sensitive to effects due to finite lattice spacing, $a$, and finite spatial volume, $N_\sigma$, is the ratio of the nucleon to the $\rho$ mass. This ratio is usually plotted as a function of the ratio $m_\pi/m_\rho$, which is a measure of the quark mass. Recall that one can choose the quark mass freely in a lattice calculation. In practice it is very difficult to perform calculations with small quark masses. One thus usually has to extrapolate to the physical quark mass value. The so-called Edinburgh plot is a way to display whether and how the experimental value $m_N/m_\rho = 1.22$ is approached when the quark mass is decreased from infinity, where $m_N/m_\rho = 3/2$ describes the static limit. This is shown in figure 7 for Wilson quarks (Allton *et al* 1992, Butler *et al* 1993, Daniel *et al* 1992, Guagnelli *et al* 1992). Similar results but with larger error bars are obtained in the staggered discretization (Cabasino *et al* 1991, Gupta R *et al* 1991a, Fukugita *et al* 1992a). Figure 7 contains (part of) the data from

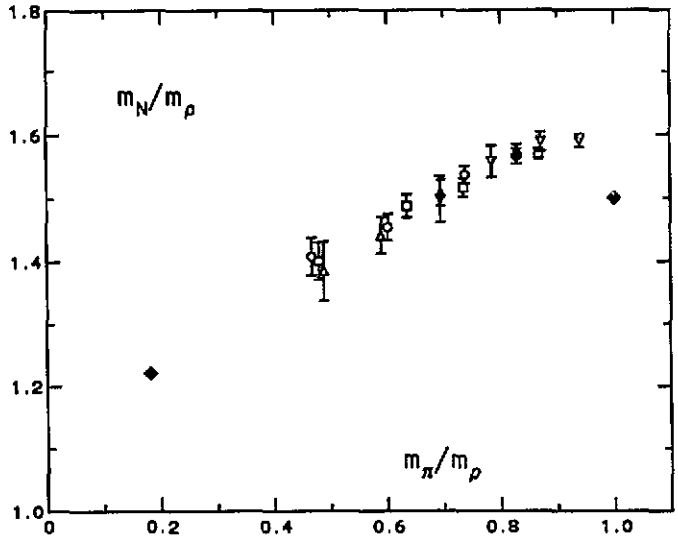


Figure 7. The Edinburgh plot for quenched Wilson fermions. The filled diamonds denote the static and the experimental result respectively.

lattices with lattice spacing $a < 0.1$ fm and $N_\sigma a \geq 2$ fm. While for $N_\sigma a \geq 2$ fm finite volume effects seem to be under control in this quantity, larger lattice spacings as well as smaller lattices shift the $m_N/m_\rho$ ratio to larger values. Although, in present lattice calculations, $m_N/m_\rho$ is always found to be larger than the experimental value, it is clear that it is decreasing as the quark mass decreases. Close to the static limit, $m_\pi/m_\rho \simeq 1$, the nucleon to ρ mass ratio is significantly above 1.5 in accordance with potential model calculations. Extrapolations to the physical pion mass produce remarkably good results. For instance, the GF11 collaboration obtains an extrapolated value of 1.28(7) which is consistent with the experimental number within 5%. (The QCDPAX collaboration (Iwasaki *et al* 1993) obtains somewhat larger $m_N/m_\rho$ ratios at small quark masses. They do not work with extended operators though but rather concentrate on studying contributions of excited states.) The close agreement is a bit surprising because below threshold, i.e. at pion masses less than $m_\rho/2$, the ρ should decay into two pions and a qualitatively new behaviour should set in. The ρ-meson decay cannot, however, be reproduced properly in the quenched approximation. Moreover, in the quenched approximation pion clouds are different from full QCD which should also effect the $m_N/m_\rho$ ratio. Current investigations with dynamical quarks (Altmeyer *et al* 1993, Bernard *et al* 1992c, Bitar *et al* 1990a, 1993, Brown *et al* 1991, Fukugita *et al* 1993, Gupta R *et al* 1991b) do not yet reach sufficiently small quark masses. Consequently, little difference to quenched results is seen so far in the currently accessible range of $m_\pi/m_\rho$ values.

As far as other low lying hadrons are concerned, the ordering of the states seems to be reproduced quite well. The precision of the numbers, however, is not quite as impressive as for the nucleon, ρ or π, although especially the results for the Δ resonance have improved considerably in the last year, $m_\Delta/m_\rho = 1.63(7)$ (Butler *et al* 1993). Another very interesting candidate is the $\eta'$ because of its relation to the $U(1)$ problem. Unfortunately, the analysis of this state requires the calculation of a quark-line disconnected diagram which is numerically utterly difficult so that so far no reliable results can be quoted.

Additional work in this area has been concerned about lattice intrinsic cross checks. In particular, finite size effects in the presence of dynamical quarks have been analysed

(Fukugita *et al* 1993, Bernard *et al* 1992c). As the staggered discretization of quark fields introduces certain flavour non-diagonal terms at finite lattice spacing it also is important to verify the restoration of flavour symmetry (Altmeyer *et al* 1993, Fukugita *et al* 1993). Likewise, at large lattice spacing the lattice causes distortions of the continuum dispersion relations. It has been shown that these effects are small at current values of the lattice spacing. Moreover, one has checked quenched Wilson fermion results by working with a variant of the Wilson action in which $O(a)$ corrections to the continuum action are reduced to $O(a^2)$ or $O(g^2a)$ (Symanzik 1983a,b, Sheikoleslami and Wohlert 1985). This should not effect the true continuum limit but it was observed that already at lattice spacings $a \simeq 0.15$ fm the improved action reproduces mass ratios which are otherwise only obtained at smaller lattice spacings, $a \leqslant 0.1$ fm. At small $a$ little difference was found. The improved action is, however, somewhat superior in the calculation of hyper-fine splittings (Allton *et al* 1992a,b, El-Khadra 1992, Lombardo *et al* 1993, Martinelli *et al* 1992).

### *3.4. Glueball spectroscopy*

A very unique topic for QCD lattice investigations is the spectrum of bound states purely made of glue, the glueballs. This is a difficult problem numerically so that the construction of suitably shaped operators (Teper 1986, Albanese *et al* 1987) with large overlaps to the lowest lying glueball states has been an important step forward technically. In combination with variational techniques it is now possible to extract reliable numbers for glueball masses. As still a very large number of independent lattice configurations is needed to obtain a sufficiently clean signal, these studies are mostly restricted to the quenched approximation. The numerical results (see the review by van Baal and Kronfeld 1989) could be tied to

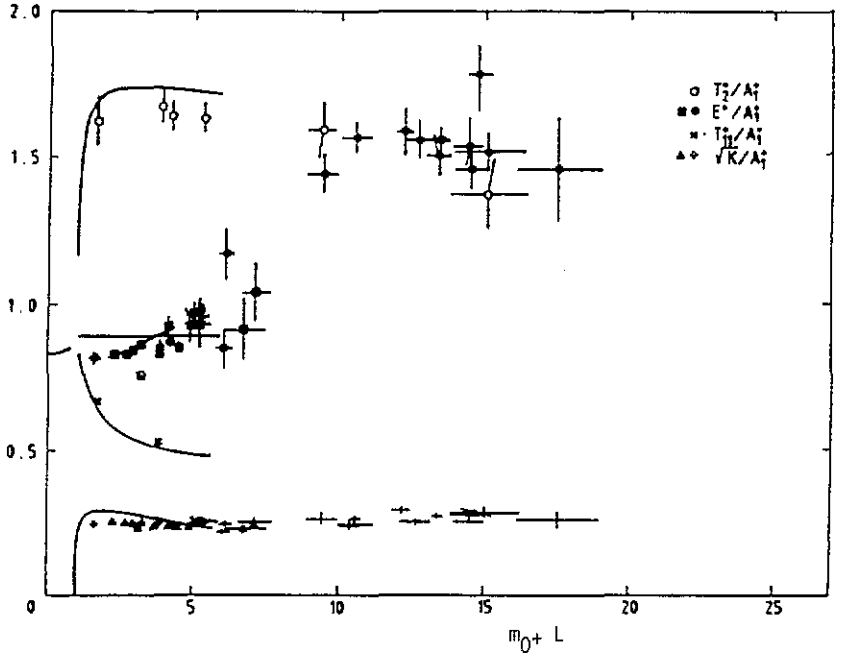


**Figure 8.** Colour $SU(2)$ data for glueball masses. $T_2^+$ and $E_2^+$ denote two different lattice representations embedded in the continuum $2^+$ representation. The masses are normalized to the $0^+$ glueball ($A_1^+$) mass. Also shown is the string tension $\sqrt{\kappa}$ and the torelon ($T_{11}^+$) mass. The solid lines are the analytic predictions. The plot is taken from (van Baal and Kronfeld 1989).

analytic calculations in small and intermediate volumes (Koller and van Baal 1988, Vohwinkel 1989) and very nice agreement was found. In particular, the apparent disagreement between results obtained from operators which belong to two different representations of the lattice rotation group which are both embedded in the same $2^{++}$ continuum representation could be resolved this way and traced back to be an effect present only in small volumes, figure 8. It is now established that the lightest glueballs are the $0^{++}$ and the $2^{++}$ states, with $m_{2^{++}} \simeq 1.5 m_{0^{++}}$ while $m_{0^{++}} \simeq 3.5\sqrt{\sigma}$ (Michael and Teper 1989). All other glueball states are heavier than 2 GeV, in particular the exotic states with quantum numbers which cannot be realized in the quark model. This is somewhat unfortunate since such a state could not mix with ordinary $\bar{q}q$ mesons and thus would give a clear experimental signal. For the non-exotic states large mixing effects can occur and are presumably strongly enhanced by virtual quark loops.

### *3.5. Weak matrix elements*

Weak interaction processes involving hadrons receive long-range QCD corrections due to the binding of quarks inside hadrons. Ambiguities in various approaches to these non-perturbative effects must be resolved in order to settle important issues as e.g. the $\Delta I = 1/2$ puzzle or the values of the Cabibbo–Kobayashi–Maskawa (CKM) mixing angles. Lattice simulations attempt to calculate the hadronic matrix elements that appear in the analyses of these questions from first principles. The required theoretical framework is quite involved because of complicated renormalizations and mixings of the operators on the lattice. Moreover, the coefficients of the renormalized lattice operators have to be related to the corresponding coefficients as calculated in some continuum renormalization scheme. This matching can be done more reliably with the perturbatively improved actions mentioned already in section 3.3 (Martinelli *et al* 1991) and improved (lattice) perturbation theory (Lepage and Mackenzie 1993). Most of the numerical calculations so far have been performed in the quenched approximation. The matrix elements studied include decay constants, form factors in semi-leptonic decays, mixing amplitudes for e.g. $K^0 - \bar{K}^0$ and non-leptonic meson decay amplitudes. Here we shall confine ourselves to a few examples.

Phenomenologically, it is quite important to resolve an ambiguity in the leptonic decay constant $f_B$ of the B meson. Analyses of $K - \bar{K}$ and $B - \bar{B}$ mixing find two solutions for $\mathcal{CP}$ violation in the CKM matrix which are distinguished by small (<150 MeV) and large (>150 MeV) values for $f_B$. The calculation of B meson amplitudes represents a technical problem on the lattice because current lattices with $1/a \leq 3.5$ GeV are rather coarse for a b quark with mass $m_b \sim 5$ GeV. In order to circumvent this difficulty one either has worked in the static approximation where the $b$ quark is held fixed in space and propagates only in time (Eichten 1988) or has simulated at various quark masses around the charm quark mass and extrapolated to the physical b quark mass (Gavela *et al* 1988a, Bernard *et al* 1988). Some results are presented in figure 9 where $\hat{f}_{PS} = f_{PS}\sqrt{m_{PS}}$ is plotted as function of the inverse mass $1/m_{PS}$ of a pseudoscalar meson. There is some ongoing discussion about certain technique details, which fortunately have only a small effect on the final results for $f_{PS}$, so that between the different groups (Gavela *et al* 1988a, Allton *et al* 1991, Alexandrou *et al* 1991, Abada *et al* 1992, Bernard *et al* 1993, Hashimoto and Saeki 1992) there seems to be agreement now that there are large corrections to the asymptotic scaling law $f_{PS}\sqrt{m_{PS}} \sim$ const, predicted to hold in the limit of infinitely heavy quarks. Moreover, if the results stay as they are, lattice QCD predicts a rather large value for $f_B$, $f_B \simeq 200 \pm 20$ MeV.

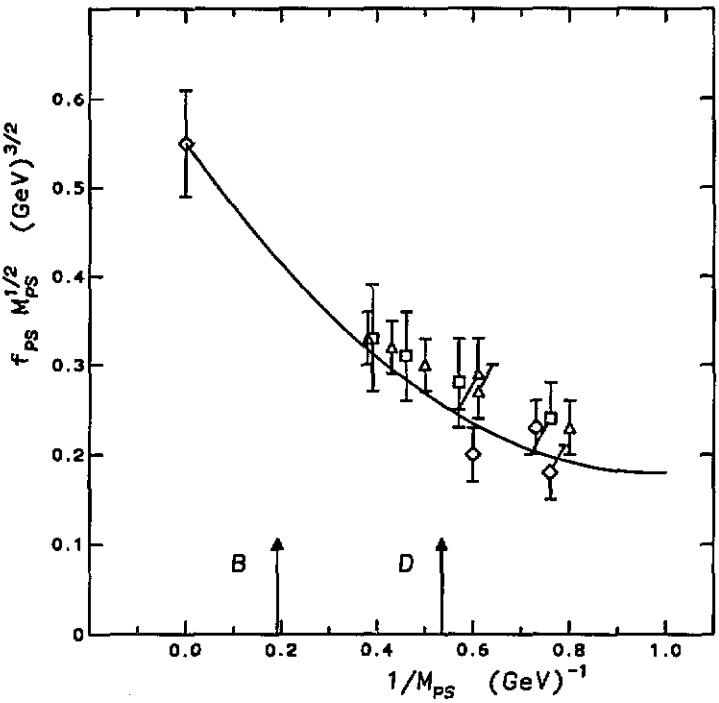


**Figure 9.** $f_{PS}\sqrt{M_{PS}}$ as function of the inverse heavy–light pseudoscalar mass, $1/M_{PS}$. The results of several calculations at various $\beta$ with propagating quarks and in the static limit are shown. The curve denotes the result of a quadratic fit to the corrections of the scaling law $f_{PS}\sqrt{M_{PS}}$ = const.

Another source of information on the CKM matrix elements are semi-leptonic decays of D and B mesons. In order to extract the mixing angles from experimental data one needs to know form factors of weak currents between the mesons. So far, lattice methods have been tested on K and D decays as a preparation for the phenomenologically more interesting B case. The matrix element is computed at several momentum transfers. Assuming pole dominance for the momentum dependence, the lattice results for $f_+(0)$ (Lubicz *et al* 1991, Bernard *et al* 1991) are in good agreement with the experimental value which is obtained by assuming $|V_{cs}| = 0.975$ (Anjos *et al* 1989, Adler *et al* 1989). For D decays into vector mesons, $D \rightarrow K^*$, the situation is more complicated. For one of the three relevant form factors, for $A_2(0)$, both the lattice investigations as well as the experimental analyses are separately contradicting each other. (Lubicz *et al* 1992) and E691 (Anjos *et al* 1990) obtain $A_2(0)$ vanishingly small while (Bernard *et al* 1992) and E653 (Kodama *et al* 1992) report a value definitely different from zero. On the lattice side, the disagreement lies not so much in the raw numerical data but in the way the extrapolations are carried out. For the other two form factors, $V(0)$ and $A_1(0)$, the two lattice studies agree more or less with each other and with experiment. In particular at the end-point of the leptons' momentum distribution, $q^2_{\max}$, both groups obtain $A_1(q^2_{\max}) \simeq 1$. It has been suggested (Bernard *et al* 1992b) to clarify the experimental situation especially at the end-point so that the unambiguous lattice prediction can be checked for systematics before the $A_2$ discrepancy is further analysed.

The kaon B parameter is defined by

$$B_K = \langle \bar{K} | \mathcal{O}^{\Delta S=2} | K \rangle / \frac{8}{3} f_K^2 m_K^2 \tag{3.8}$$

where the denominator is the vacuum saturation value. $B_K$ is related to the $\mathcal{CP}$ violation parameter $\epsilon$ in the $K^0$ system and a determination of $B_K$ allows constraints on the mixing angles and the top mass. The kaon $B$ parameter has been calculated both for the Wilson (Gavela *et al* 1988b, Bernard and Soni 1990, Gupta R *et al* 1993) and the staggered (Sharpe *et al* 1992b) discretization of the quark action. Rather accurate results could be obtained in the latter scheme because a continuous chiral symmetry on the lattice protects the operator from mixing with operators of left-right chiral structure. These mixings do occur for the Wilson case and have to be subtracted. The results for the two discretization schemes show reasonable agreement. There are sizable $O(a)$ corrections which have been studied during the last two years, the result being that $B_K \simeq 0.6$ in the limit $a \to 0$. The analyses have been repeated in full QCD now (Kilcup 1991, Fukugita *et al* 1992b), with little difference to the quenched results being seen.

Finally, a number of attempts have been made to compute the $K \to \pi\pi$ amplitudes in order to understand the $\Delta I = 1/2$ rule and to constrain the $\mathcal{CP}$ violating angle in the CKM matrix through the parameter $\epsilon'$. Despite some original optimism, these quantities have proven hard to extract from the lattice. The $\Delta S = 1$ four quark operators mix with a number of operators with lower dimension. Their contributions have to be subtracted non-perturbatively which has turned out to be difficult numerically. For staggered quarks with their chiral properties the situation is somewhat better. Here one can use chiral perturbation theory to relate the $K \to \pi\pi$ amplitudes to those for $K \to \pi$ and $K \to$ vacuum and fix the subtractions by chiral symmetry. Still, the contributions of so-called eye-operators are not stable numerically. The main problem, however, is that whether one computes $K \to \pi\pi$ or $K \to \pi$, one has to deal with final state $\pi\pi$ interactions. This is difficult. It has been shown (Maiani and Testa 1990) that one cannot just put two pions with non-zero momentum on a Euclidean lattice and expect them to represent an 'out' state. So one is beginning to first investigate $\pi\pi$ systems (Guagnelli *et al* 1990, Sharpe *et al* 1992) before one can come back to the original problem.

## 4. QCD at high temperature

### *4.1. A new phase of matter*

One of the outstanding predictions of QCD, which still awaits its experimental verification, is the existence of a new phase of strongly interacting matter at high temperatures and/or densities—the quark gluon plasma (QGP): at temperatures of the order of the pion mass, $T \sim 140\,\mathrm{MeV}$, or densities a few times that of ordinary nuclear matter, $n \sim (3-5)n_0$, with $n_0 = 0.15\,\mathrm{fm}^{-3}$, conditions are reached where hadrons start overlapping and the interaction among the internal partonic degrees of freedom, described by QCD, becomes important. Theoretical investigations of this complicated transition regime, in particular the phase transition itself, clearly require non-perturbative techniques. However, somewhat surprisingly, it turned out that such an approach is important also in the high temperature phase. Despite asymptotic freedom a perturbative description of the plasma phase itself is not at all obvious; the perturbative expansion is plagued by infra-red divergences (Polyakov 1979, Linde 1980 and Kapusta 1979), which become worse with increasing order of the expansion. In particular, one finds that in the gluon propagator an electric screening mass of $O(gT)$ and a magnetic screening mass of $O(g^2T)$ have to be generated dynamically in order to render the expansion of thermodynamic quantities finite. These mass gaps signal the existence of different length

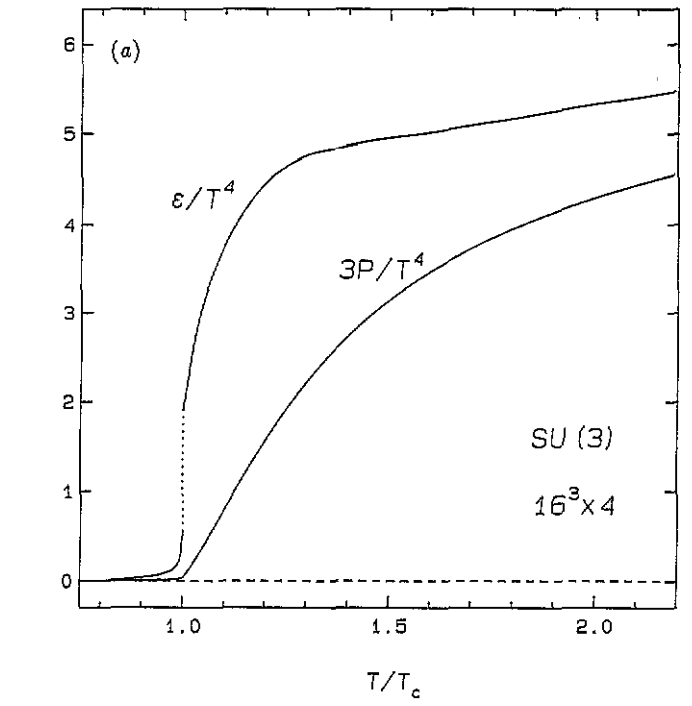


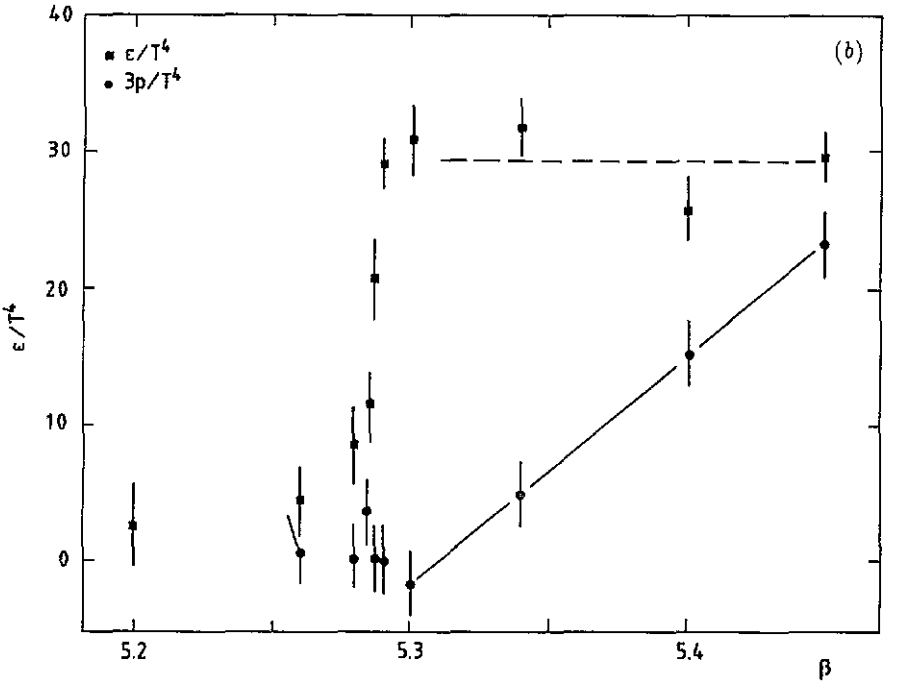


**Figure 10.** In (*a*) energy density and pressure of an $SU(3)$ gauge theory in units of $T^4$ are shown as a function of $T/T_c$. The curves have been obtained from an integration of data for the free energy density (Engels *et al* 1990a). Violations of asymptotic scaling have been taken into account. In (*b*) the same quantities are shown for two flavour QCD (Gottlieb *et al* 1987d). So far no attempt has been made to correct for scaling violations in this case.

scales in the plasma phase. In addition to the characteristic perturbative length scale, $l_P \sim 1/T$, a hierarchy of non-perturbative length scales like the electric ($l_E$) and magnetic ($l_M$) mass gap show up,

$$\begin{aligned} l_P < l_E < l_M, \\ 1/T < 1/gT < 1/g^2T, \end{aligned} \tag{4.1}$$

and thus limit the applicability of perturbation theory. A perturbative treatment of long-distance properties of the QCD plasma phase seems to be impossible. In fact, the above relations led to doubts about any perturbative treatment of the high temperature phase in terms of quarks and gluons as basic excitations, and it has been suggested that a description in terms of colourless quasi-particles may be more appropriate (DeTar 1988).

Different physical observables are sensitive to different momentum regimes. They thus may be influenced differently by the various length scales. This, for instance, shows up already in the equation of state (EOS). While the energy density rapidly approaches ideal gas behaviour, the pressure shows very strong deviations up to temperatures $T \sim (2-3)T_c$. Some results for the EOS of a pure $SU(3)$ gauge theory (Engels *et al* 1990a) and two flavour QCD (Gottlieb *et al* 1987d) are shown in figure 10. We note that although the phase transition is first order in the case of quenched QCD (pure gauge theory) also the energy density decreases strongly close to $T_c$. This leads to a rather small latent heat of the transition. Measured in units of the energy density of an ideal gluon gas, $\epsilon_{SB}$, one finds (Engels *et al* 1990a, Iwasaki *et al* 1991, 1992)

$$\frac{\Delta\epsilon}{\epsilon_{SB}} = 0.315 \pm 0.030. \tag{4.2}$$

Using, for the critical temperature of the deconfinement transition in the $SU(3)$ gauge theory, a value of $T_c \simeq 235\,\mathrm{MeV}$ (from table 1) yields $\Delta\epsilon \simeq 635\,\mathrm{MeV\,fm^{-3}}$ for the latent heat.

### *4.2. Deconfinement*

Physically it is rather tempting to relate the finite temperature QCD phase transition to the deconfinement mechanism. Quarks and gluons are confined at low temperature and form colourless hadrons. These may break up at high temperatures and the partons become free, i.e. deconfined. This picture can be made rigorous in pure $SU(N)$ gauge theories, where dynamical quarks are absent. Dynamical quarks will spoil the strict notion of confinement even at zero temperature as quark–antiquark pair creation will lead to a flat heavy quark potential at large distances. The potential thus would not be confining in the strict sense.

Pure $SU(N)$ gauge theories have a global $Z(N)$ symmetry, which controls the properties of the finite temperature transition. If one performs a global $Z(N)$ rotation of all timelike gauge fields $U_0(n)$ originating from the sites $n=(n_0,\boldsymbol{n})$ of a given temporal hyperplane (fixed $n_0$) of the lattice,

$$U_0(n_0, \boldsymbol{n}) \rightarrow U_0'(n_0, \boldsymbol{n}) = zU_0(n_0, \boldsymbol{n}) \qquad z \in Z(N),\ n_0 \text{ fixed} \tag{4.3}$$

the action remains unchanged, $S_G(\{U_\mu'(n)\}) = S_G(\{U_\mu(n)\})$. In contrast, the Polyakov loop,

$$L_{\boldsymbol{n}} = \prod_{n_0=1}^{N_\tau} U_0(n_0, \boldsymbol{n}) \tag{4.4}$$

which describes the propagation of a static fermionic test charge and probes the screening properties of the surrounding gluonic medium, transforms non-trivially under this transformation,

$$L(\boldsymbol{n}) \rightarrow zL(\boldsymbol{n}) \qquad z \in Z(N). \tag{4.5}$$

Its expectation value, $\langle L(\boldsymbol{n})\rangle$, thus will vanish as long as the theory preserves the global $Z(N)$ symmetry. It will, however, acquire a non-vanishing value if this symmetry is spontaneously broken.

It is expected that the critical properties of $(d+1)$-dimensional gauge theories are described by an effective $d$-dimensional spin model given in terms of the Polyakov loop. Critical indices should then only be determined by the dimensionality of the spin system and its global $Z(N)$ symmetry (Svetitsky and Yaffe 1982a, b). In fact, there is strong evidence from numerical simulations that the phase transition for $SU(2)$ gauge theory is of second order and in the same universality class as the 3D Ising model, whereas the $SU(3)$ gauge theory leads to a first order transition, as expected on the basis of these general universality arguments.

The critical properties at the transition point have been studied in detailed finite size scaling studies, which allow a rather accurate determination of critical indices. In figure 11 we show the result of such a scaling analysis for the critical exponent $\nu$ of $SU(2)$ (Engels *et al* 1990b) and $SU(3)$ (Fukugita *et al* 1990) gauge theories. In particular one finds:

$$SU(2): \frac{\beta}{\nu} = 0.545 \pm 0.030 \qquad \frac{\gamma}{\nu} = 1.93 \pm 0.03 \qquad \nu = 0.65 \pm 0.04$$

$$SU(3): \frac{\gamma}{\nu} = 3.02 \pm 0.14 \qquad \nu = 0.34 \pm 0.01.$$

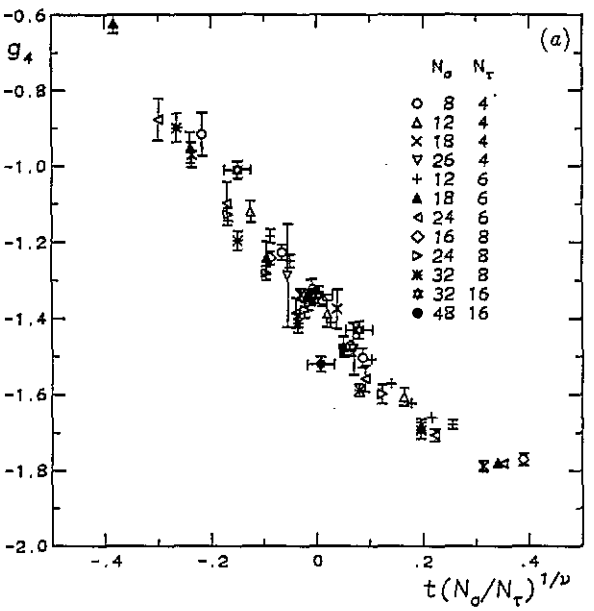


**Figure 11.** Determination of the critical exponent $\nu$ for the $SU(2)$ deconfinement transition obtained from a finite size scaling analysis of the order parameter (Engels *et al* 1990b) (*a*). In (*b*) the finite size scaling of the critical coupling is shown. This leads to a determination of the ratio of critical exponents, $\gamma/\nu$, for the $SU(3)$ gauge theory (Fukugita *et al* 1990).

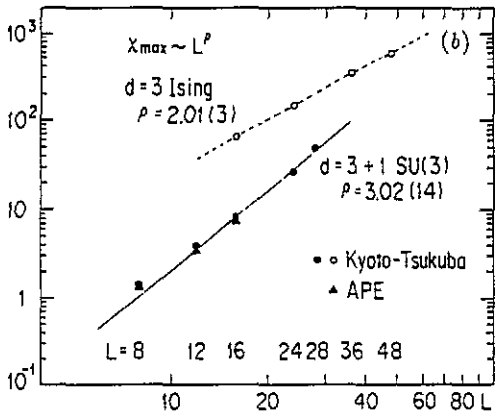


While the exponents for $SU(2)$ are in agreement with those of the three dimensional Ising model, $\beta/\nu = 0.516(5)$, $\gamma/\nu = 1.965(5)$, $\nu = 0.63(3)$, the result for $SU(3)$ is consistent with $\nu = 1/3$, $\gamma = 1.0$, which is expected for a first order phase transition in 3 dimensions.

Further insight into the nature of the phase transition in the pure gauge sector of QCD comes, for instance, from the temperature dependence of the heavy quark potential. This is expected to change from a linearly arising confinement potential to a Debye screened (Yukawa) potential at high temperatures

$$V(r,T) = \begin{cases} \frac{-\alpha(T)}{r} + \sigma(T)r & T < T_c \\ \frac{-\alpha(T)}{r}\exp\{-m_D(T)r\} & T > T_c \end{cases} \tag{4.6}$$

The numerical studies indicate that indeed the string tension decreases as one approaches $T_c$. Furthermore, the confining part of the potential disappears above $T_c$ and one is left with a screened Coulomb potential. Some results for the screening mass,

$$\mu = \begin{cases} \sigma(T)/T & T < T_c \\ m_D(T) & T > T_c \end{cases} \tag{4.7}$$

are shown in figure 12 (Fukugita *et al* 1989, Brown *et al* 1988, Bacilieri *et al* 1988). We note that at $T_c$ the correlation length, $\xi = 1/\mu$, in the pure $SU(3)$ gauge theory is $\simeq (1-2)T_c^{-1}$, i.e. about (1–2) fm. This shows that close to $T_c$ the system still is strongly correlated. However, as can be seen from figure 12, already at temperatures $T \simeq 1.5T_c$ the screening mass is close to the leading order perturbative value

$$m_D(T) = \left(\frac{N}{3} + \frac{n_f}{6}\right)^{1/2} g(T)T \qquad T \gg T_c. \tag{4.8}$$

In accordance with this perturbative result one finds that the screening mass increases substantially, if dynamical quarks are present in the medium (Karsch and Wyld 1988, Unger 1992). This efficient screening of the heavy quark potential has important consequences for the formation of heavy quark bound states in the high temperature phase (Karsch *et al* 1988) which has been conjectured as a possible signal for quark–gluon plasma formation in heavy ion collisions (Matsui and Satz 1986).

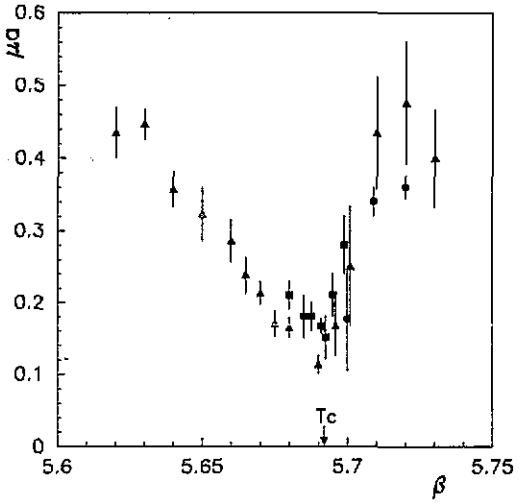


**Figure 12.** Screening masses in units of the lattice spacing for the pure $SC(3)$ gauge theory obtained on lattices of size $4 \times 24^3$ (squres) (Fukugita *et al* 1989) (dots) (Brown *et al* 1988) and $4 \times 8^2 \times 32$ (triangles) (Bacilieri *et al* 1988).

### *4.3. The chiral phase transition*

Phase transitions are usually related to the breaking of global symmetries of the Lagrangian. Besides a global $U(1)$ symmetry corresponding to baryon number conservation the QCD Lagrangian has, in the limit of vanishing quark masses, a global chiral flavour symmetry, $SU_L(n_f) \times SU_R(n_f)$. At low temperatures the chiral flavour symmetry is spontaneously broken and it is expected that it gets restored at high temperatures. In the limit of vanishing quark masses this symmetry will control the properties of the QCD phase transition. The expected critical behaviour has been discussed some time ago by Pisarski and Wilczek (Pisarski and Wilczek 1984). On the basis of a renormalization group analysis of the most general 3D effective chiral Lagrangian they showed that the generic chiral transition is expected to be first order as long as $n_f \geqslant 3$. In the most interesting case of two massless flavours, however, the RG-analysis does not lead to a decisive answer—a first as well as a second order transition is possible. In the two flavour case the axial $U(1)$ symmetry, which at zero temperature is broken due to the axial anomaly, plays an important role. If this symmetry gets effectively restored at the chiral transition point, a first order transition is possible also in the two flavour case. Otherwise the transition would be second order with critical indices of the $O(4)$ Heisenberg model (Pisarski and Wilczek 1984, Wilczek 1992).

Studies of the chiral transition on the lattice suffer from the fact that one does not have a lattice formulation with the same symmetry properties as the continuum action at hand. Most studies so far have been performed with the staggered fermion action, which, for $\bar{f}$ species of staggered fermions, is invariant only under a $U(\bar{f}) \times U(\bar{f})$ subgroup of the full flavour symmetry group. Due to species doubling these $\bar{f}$ species of staggered fermions give rise to $n_f = 4\bar{f}$ quark flavours in the continuum limit. Only in this limit does one recover a fermionic theory which has the correct $SU(4\bar{f}) \times SU(4\bar{f})$ chiral symmetry. The order parameter for this lattice chiral symmetry is given by the chiral condensate,

$$\langle \bar{\chi}\chi \rangle = \frac{1}{N_\tau N_\sigma^3} \frac{\partial}{\partial m} \ln Z. \tag{4.9}$$

The importance of the different symmetry properties of the lattice and continuum Lagrangian is evident in the case of $\tilde{f} = 1$, which corresponds to 4-flavour QCD in the continuum limit. The lattice Lagrangian in this case only has a $U(1) \times U(1)$ symmetry, which is isomorphic to $O(2)$. One thus expects a second order phase transition, with the critical exponents of the 3D $O(2)$ spin models as long as the flavour symmetry is strongly broken and the lattice symmetry group controls the dynamics. In the continuum limit, on the other hand, one expects to find a first order phase transition. This change in critical behaviour has indeed been observed in numerical simulations. In the strong coupling limit the four flavour theory has a second order phase transition (Boyd *et al* 1992a), while already at intermediate values of the gauge coupling ($g^2 \simeq 1$) the transition is clearly first order (Gupta *et al* 1986, Karsch *et al* 1987, Gavai *et al* 1990).

The four flavour theory has been studied for various values of the quark mass. These studies suggest that in the continuum limit there will be a line of first order transitions connecting the zero-quark mass chiral transition with the deconfinement transition in the limit $m \to \infty$ (Gupta R *et al* 1986). The situation for $n_f < 4$ seems to be different, although these studies can, at present, not be considered as complete. In particular, one cannot rule out that the order of transitions might change closer to the continuum limit, as we have discussed above. The present understanding of the phase diagram for three dynamical quarks with different masses is illustrated in the generic phase diagram shown in figure 13 (Brown *et al* 1990). Whether the regions of first order transitions in the vicinity of the chiral ($m_i = 0$) and quenched ($m_i \to \infty$) limits are really disjoint and whether the physically interesting case of two light quarks, $m_u \simeq m_d \simeq 0$, and a heavier strange quark, $m_s \simeq 150\,\mathrm{MeV}$, will lead to a first or second order transition is currently subject of intensive research activities (Petersson 1993).

Recently, first indications have been reported that a change in the order of the transition might occur in two flavour QCD (Mawhinney 1993, Petersson 1993), similar to what has

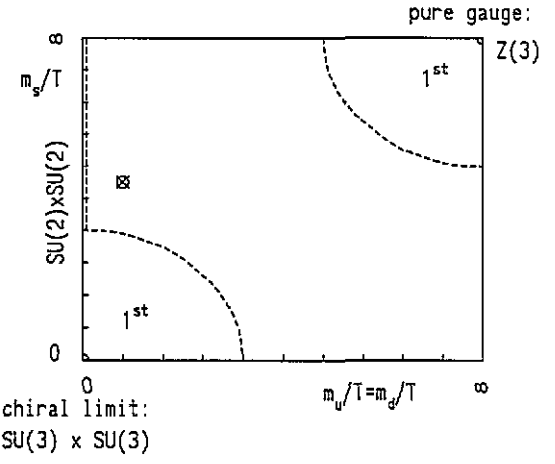


**Figure 13.** Generic phase diagram for three flavour QCD (Brown *et al* 1990). The arcs enclose regions of first order phase transitions. The dashed lines indicate lines of 2nd order phase transitions. On the $m_u = 0$ axis this has been displaced a bit for better visibility. The crossed circle indicates the location of the physical strange to up quark mass ratio. Present Monte Carlo simulations suggest that this point lies outside the first order region. However, this still has to be verified on larger lattices.

been found in the four flavour case. Due to this unsatisfactory situation it will be increasingly important to reach consistent conclusions on the order of the transition by using different lattice regularizations for the fermions. Studies of the chiral transition with Wilson fermions are difficult, as the lattice Lagrangian has no continuous chiral symmetry and the properties related to the chiral flavour symmetry, which are so important for the discussion of phase transitions, can only be recovered in the continuum limit. Consequently the indications for a finite temperature phase transition with Wilson fermions show, at least for small values of $N_\tau$ and thus at rather strong coupling, the features of a continuous crossover behaviour rather than a genuine phase transition (Fukugita *et al* 1986, Gupta R *et al* 1989, Bitar *et al* 1990b, 1991). Recent investigations of two flavour QCD with Wilson fermions for $N_\tau = 6$ suggest, however, a sharpening of the crossover behaviour, when one comes deeper into the regime of small lattice spacings. These studies even leave the possibility for the existence of a first order phase transition (Bernard *et al* 1992g). They certainly have to be pursued in the future. The determination of the transition temperature for Wilson as well as staggered fermions also suggests that with increasing $N_\tau$ the results extracted in both regularization schemes start approaching each other.

A consequence of the spontaneously broken chiral symmetry in QCD is the existence of a massless Goldstone boson, the pion, as well as the non-degeneracy of the masses of chiral partners. These properties of the hadron spectrum should change in the chirally symmetric high temperature phase. The appropriate quantity to analyse on the lattice in this case is the large distance behaviour of spacelike correlation functions for operators with hadronic quantum numbers, $H(\boldsymbol{n}, n_3)$ (DeTar and Kogut 1987a),

$$G_s^H(n_3, \tilde{\boldsymbol{p}}) = \frac{1}{N_\tau N_\sigma^3} \sum_{\tilde{n}=(n_0,n_1,n_2)} e^{i\tilde{p}\tilde{n}} \langle H(\tilde{n}, n_3) H^\dagger(\tilde{0}, 0) \rangle. \tag{4.10}$$

At large spatial separations these operators yield a screening length, characteristic for the corresponding quantum number channels. As long as there exist bound states in a given quantum number channel the screening length will give the mass of the lowest lying state. We will discuss this in more detail in the next subsection. In figure 14 we show some results obtained in the staggered fermion formulation for (pseudo)scalar and (pseudo)vector meson channels as well as for the baryon channel (DeTar and Kogut 1987a,b, Gottlieb *et al* 1987c, Born *et al* 1991b, Boyd *et al* 1992b). The change in chiral properties of QCD is clearly visible in this figure. All the chiral partners yield degenerate screening masses above $T_c$. Similar results have been obtained with Wilson fermions (Bitar *et al* 1991).

### *4.4. Spatial correlations in the quark–gluon plasma*

As discussed in section 4.1, the high temperature phase of QCD is most certainly not simply described by a weakly interacting gas of quarks and gluons. In particular, in the vicinity of $T_c$ non-perturbative effects will modify the spectrum strongly. We have discussed the effect on the equation of state and the Debye screening lengths in the previous sections. A controversial issue is the interpretation of so-called spatial correlation functions. These are not readily related to physical observables and (sometimes) show a behaviour which is not easily understood in terms of ordinary high temperature perturbation theory.

The behaviour of the spatial hadronic correlation functions, defined in (4.10), can be analysed in terms of the spectral representation of these correlation functions. At low temperatures the spectral functions have poles corresponding to the (temperature dependent) masses of hadrons with the given quantum numbers. In the high temperature limit, however,

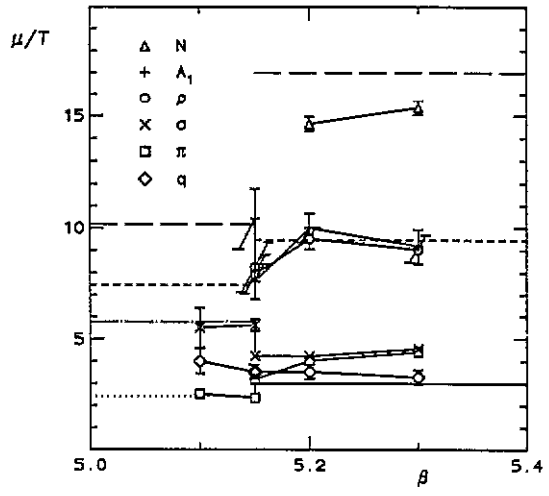


**Figure 14.** Screening masses $\mu_i/T$ as a function of $\beta$ for $n_f = 4$ from an $8 \times 16^3$ lattice. The state denoted 'q' gives the screening mass extracted from the quark propagator in Landau gauge (Boyd *et al* 1992b). Lines to the left give the values of the zero temperature masses in units of $T_c$ calculated at $\beta = 5.15$; $m_\pi/T_c$ (dotted), $m_\sigma/T_c$ (dashed-dotted), $m_\rho/T_c$ (short dashes), and $m_N/T_c$ (long dashes). Lines to the right give screening masses corresponding to free quark propagation in the quark (solid), mesonic (short dashes) and baryonic (long dashes) channels.

the spectral function may only have a cut, corresponding to the free propagation of the minimal number of partons in the hadronic channel considered, i.e. two for mesonic and three for baryonic operators. The cut will start at the lowest possible momentum, $\vec{p}_{\min} = (p_{0,\min}, 0, 0, 0,)$, which due to anti-periodic boundary conditions for the fermions is given by the lowest Matsubara frequency,

$$p_{0,\min} = \begin{cases} 2\pi T & \text{meson operators} \\ 3\pi T & \text{baryon operators} \end{cases} \tag{4.11}$$

The screening masses for spatial hadronic operators thus are expected to approach the lowest possible Matsubara frequency in the high temperature limit, $\mu \sim p_{0,\min}$. This is indeed the case for the baryonic, (pseudo)vector and also quark quantum number channels, as can be seen in figure 14. An exception is the (pseudo)scalar screening mass. This clearly deviates strongly from the free field behaviour and also cannot be understood in terms of small perturbative corrections. Investigations of the quark mass dependence of the scalar screening mass suggest, however, that this screening mass is not associated with a bound state but rather reflects the still rather strong attractive interactions in this channel (Gupta S 1992b).

Spatial hadronic correlation functions are in so far rather simple as their high temperature behaviour can be studied and understood in terms of high temperature perturbation theory. This is not the case for the behaviour of other spatial observables like spatial Wilson loops or spatial four-point correlation functions. The former still show area law behaviour in the high temperature phase (Borgs 1985, Manousakis and Polonyi 1987) and thus give rise to a non-perturbative, spatial 'string tension'. The occurrence of such a string tension can be understood by means of dimensional reduction (Appelquist and Pisarski 1981) of a quantum field theory at high temperature. For QCD the integration over static modes leads, in the high temperature limit, to an adjoint Higgs model in three dimensions which shows confining properties for the spatial gauge degrees of freedom, although the potential between the timelike gauge fields (Higgs fields) is screened. The short distance properties of this

effective model have been studied in perturbation theory (Reisz 1991, 1992, Lacock *et al* 1992) and can be related to the short distance properties of QCD at high temperatures. However, in how far the large distance properties of the effective theory describe the large distance properties of QCD, is at present unknown and deserves more detailed studies. As the non-static modes do not decouple completely in the high temperature limit (Landsman 1988), it is to be expected that the effective theory becomes increasingly complicated, if it should describe also the large distance properties of QCD.

Even less understood is, at present, the behaviour of point-splitted quark four-point functions, which at zero temperature are used to study hadronic wave-functions. At finite temperature their physical interpretation is not at all obvious (Bernard *et al* 1992e). The spatial 'wave-functions' calculated for various quantum number channels still are strongly localized while leading order perturbation theory would have suggested very broad 'wave-functions'. It is not clear whether these calculations indicate that there are localized 'quasi'-particles with the quantum numbers of e.g. a pion or a baryon in the high temperature phase. Most likely this is not the case. Various measurements of physical quantities like the baryon number susceptibility (Gottlieb *et al* 1987d, 1988) or the baryon number distribution in the vicinity of static quark sources (Bernard *et al* 1992f) suggest that quarks can move quite freely in the high temperature phase.

## 5. Electro-weak sector of the standard model

The Glashow–Salam–Weinberg theory is very successful in describing electro-weak interactions. Experimentally, there are no signs of its breakdown. Still, from a theoretical point of view, the theory is not satisfactory. Besides the number of free parameters being large, neither the Higgs sector nor the $U(1)$ gauge subgroup present asymptotically free theories. This indicates their breakdown at large energies (couplings). One of the main motivations for lattice studies of the standard model has therefore been to possibly quantify its limitations as a consistent quantum field theory by analysing it at a non-perturbative level or to detect deviations from the perturbative Callan–Symanzik β-functions which would lead to a different behaviour in the large cut-off limit.

### *5.1. Pure Higgs systems*

In the electro-weak sector of the standard model, the $SU(2)_L \times U(1)_Y$ gauge couplings are small at the $m_W$ scale. Likewise, except for a very large top quark mass, the Yukawa couplings of the quarks are also small. Thus, at least in a first approximation, one may ignore gauge fields and fermions and concentrate on the Higgs sector alone. This is then an $O(4)$ invariant scalar field theory,

$$\mathscr{L} = \frac{1}{2}(\partial_\mu \Phi)^2 + \frac{1}{2} m_0^2 \Phi^2 + \frac{g_0}{4!} \Phi^4. \tag{5.1}$$

In a (semi)classical treatment, the Higgs mechanism is based on the observation that for $m_0^2 \leqslant 0$ a minimum value for the action is obtained when the Higgs field acquires a non-vanishing value. This leads, in the unitary gauge, to a gauge boson mass of

$$m_W^2 = \frac{1}{4} g_L^2 \langle \Phi \rangle^2 \tag{5.2}$$

where $g_L$ is the renormalized $SU(2)_L$ gauge subgroup coupling and $\langle\Phi\rangle$ represents the Higgs field expectation value in the vacuum. This relation remains valid for arbitrarily large Higgs self-couplings $g$ as long as the gauge coupling can be treated perturbatively (Dashen and Neuberger 1983). On the other hand, the mass of the Higgs boson is given by

$$m_H^2 = \frac{1}{3} g_R \langle\Phi\rangle^2. \tag{5.3}$$

Here, the renormalized quartic coupling $g_R$ enters crucially. In particular, by means of a combination of strong-coupling expansion and renormalization techniques it was shown (Lüscher and Weisz 1987, 1988, 1989) that in 4 dimensions scalar field theories are trivial, i.e. the renormalized quartic coupling vanishes when the ultraviolet cut-off is taken to infinity. Further investigations at small gauge coupling, perturbative calculations as well as numerical lattice simulations, confirmed that the triviality is not destroyed when $SU(2)$ gauge fields are reintroduced (Hasenfratz A and Hasenfratz P 1986, Langguth and Montvay 1987, Hasenfratz A and Neuhaus 1988, Bock *et al* 1990a). A non-trivial fixed point at intermediate values for the gauge coupling is not entirely excluded but its existence seems unlikely because the Higgs phase-transition line appears to be first order everywhere, in agreement with the original work of Coleman and Weinberg (Coleman and Weinberg 1973). Thus, the standard model should be the effective low-energy limit of some larger theory, valid below an energy scale set by an intrinsic cut-off $\Lambda$. Equation (5.3) then implies an upper bound on the Higgs mass: a given value for the momentum cut-off leads to a maximum value for the coupling $g$ which decreases further $\Lambda$ is increased. The quantitative

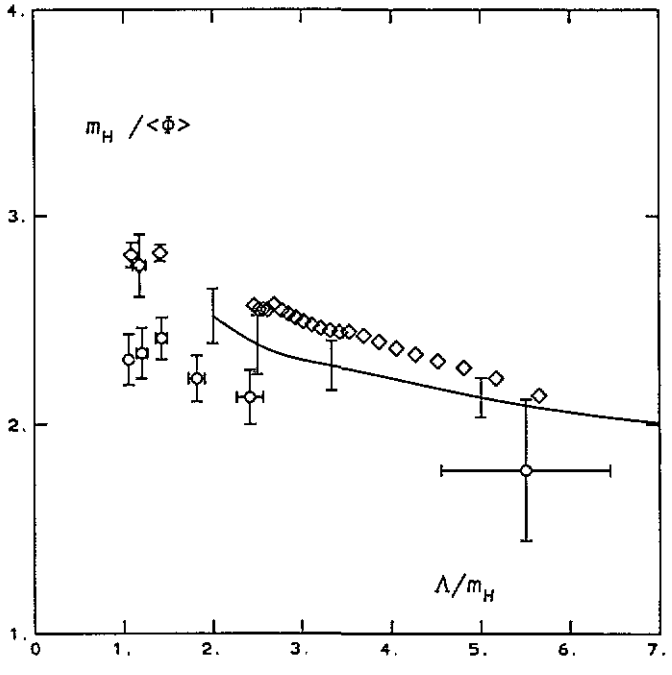


**Figure 15.** Upper bound on the ratio $m_H/\langle\phi\rangle$ in the pure Higgs sector. The data are obtained with the standard action (diamonds) (Hasenfratz A *et al* 1987, Göckeler *et al* 1993) and on simplicial lattices (circles) (Bhanot *et al* 1990). The curve denotes the analytic result (Lüscher and Weisz 1989) for the standard action with the estimated theoretical uncertainty indicated by error bars. As the cut-off definition, $\Lambda = 1/a$ has been adopted.

determination of the bound on the Higgs mass can in principle require a non-perturbative treatment because $g$ does not need to be small for small values of the cut-off. This question has been addressed both by analytical calculations (Lüscher and Weisz 1987, 1988, 1989) and numerical simulations (Hasenfratz A *et al* 1987, Kuti *et al* 1988). The analysis has been refined since then, in particular in regard to finite-size effects due to the presence of massless Goldstone-bosons in the symmetry breaking phase (Neuberger 1988, Hasenfratz P and Leutwyler 1990, Hasenfratz A *et al* 1990, Göckeler *et al* 1993). Some results are shown in figure 15. Moreover, the universality of the upper bound has been investigated, i.e. the dependence of the Higgs mass on the specific lattice discretization scheme has been checked (Bhanot *et al* 1990, Göckeler *et al* 1993). Differences of $m_H/\langle\phi\rangle$ between various lattice regularization schemes are not too surprising as the cut-offs in physical units are different. Moreover, the finite result for the upper bound depends on the physical criterion which specifies how much cut-off dependence is allowed in what physical quantity. A popular choice has been the somewhat *ad hoc* condition $\Lambda > 2m_H$. Another procedure utilizes the 90° WW scattering cross section (Bhanot *et al* 1990, Göckeler *et al* 1993). Correspondingly, the results exhibit a 10–20% variation. Nevertheless it is quite clear that a Higgs mass larger than 600(60) GeV cannot be accommodated by the standard model. This number is consistent with the perturbative unitarity bound of $m_H < 800\,\text{GeV}$ (Lee *et al* 1977). The reason is that even for a low cut-off, $\Lambda = m_H$, the renormalized quartic Higgs self-coupling is not large. Yet it is reassuring, that the perturbative estimate is under non-perturbative control.

### *5.2. The Higgs phase transition*

The spontaneously broken symmetry in the Higgs field sector of the standard model is expected to be restored at high temperature (Kirzhnits and Linde 1972, Weinberg 1974). The order parameter for this phase transition is the expectation value of the Higgs field, $\langle\Phi\rangle$, which at zero temperature takes on the value, $\langle\Phi\rangle \simeq 250\,\text{GeV}$. The perturbative calculation of the effective Higgs potential becomes rather involved, once higher order corrections as well as the influence of the Higgs and W-boson masses are taken into account (Dine *et al* 1992, for a recent review see also Kripfganz 1992). The transition turns out to be first order with a critical temperature given by,

$$T_{SR} \simeq \sqrt{\frac{2}{3}}\,\langle\Phi\rangle\,\frac{m_H}{m_W}. \tag{5.4}$$

The transition is weakly first order as the discontinuity in the order parameter turns out to be much smaller than the transition temperature itself,

$$\langle\Phi\rangle(T_{SR}) \simeq \frac{m_W^3}{m_H^2\langle\Phi\rangle(0)}\,T_{SR}. \tag{5.5}$$

The occurrence of a symmetry restoring phase transition has been established in numerical simulations of the $SU(2)$-Higgs model at finite temperature (Evertz *et al* 1987, Damgaard and Heller 1988) and the recent calculations in the region of small quartic Higgs coupling (Bunk *et al* 1992) suggest that this transition indeed is first order. These latter calculations aim, for the first time, at a quantitative determination of the critical temperature in a parameter regime where the Higgs boson mass is approximately equal to the W-boson mass. It has been found that the discontinuity in the Higgs condensate at $T_{SR}$ is about twice

as large as expected from perturbation theory, $\langle\phi\rangle_R(T_{SR}) \simeq 0.68T_{SR}$. The critical temperature itself has been estimated as

$$T_{SR} \simeq 1.74m_W \simeq 140\text{GeV}. \tag{5.6}$$

In the absence of gauge degrees of freedom, i.e. in the $O(4)$ symmetric Higgs sector defined by (5.1), the Higgs phase transition has been analysed numerically using finite size scaling techniques (Jansen and Seuferling 1990). Here it has been found that the critical parameter of the transition is in good quantitative agreement with predictions based on renormalized perturbation theory (Lüscher and Weisz 1989). This should not be too surprising as the studies at zero temperature have indicated that the renormalized quartic Higgs coupling never becomes large. Consequently the perturbative estimates for the Higgs phase transition are also expected to be rather accurate. In the $O(4)$ model one finds for the critical temperature $T_{SR} \simeq \sqrt{2}\langle\phi\rangle_R$. This is consistent with a determination of a lower bound for the symmetry restoration temperature (Gavai *et al* 1992), which can be deduced from the upper bound for the Higgs boson mass, discussed in the previous section. One finds as a lower bound

$$\frac{T_{SR,\min}}{m_H} = 0.58 \pm 0.02, \tag{5.7}$$

when the Higgs mass reaches the cut-off, i.e. $m_H a = 0.5$. Using for the Higgs mass the upper bound $m_H < 600\text{MeV}$, one thus obtains $T_{SR,\min} = 350\text{GeV}$ as a lower bound for the symmetry restoration temperature in the $O(4)$ model. This is more than a factor two larger than the value found for the transition temperature in the simulation of the $SU(2)$ Higgs model. In the future it thus will be important to understand in more detail the dependence of $T_{SR}$ on the parameters of the model, in particular its dependence on $m_H$ and $m_W/m_H$.

### *5.3. Higgs–Yukawa couplings*

Higgs–Yukawa couplings of heavy quarks to the Higgs field are interesting for several reasons. The presence of heavy quarks could affect the upper bound on the Higgs mass. Secondly, from the triviality of Higgs–Yukawa couplings, upper bounds on heavy quark masses can be derived much like in pure Higgs systems. Finally, from a general field theoretical point of view, it is a challenge to put chiral fermions on the lattice. Phenomenologically, this is of principal importance if there is a strongly interacting sector with chiral fermions in theories with larger symmetry groups than in the standard model.

The problem of treating chiral fermions in the lattice regularization consists in the occurrence of the so-called doubler fermions. If one discretizes the Dirac action additional fermions are generated such that the number of left- and right-handed fermions is equal. As mentioned in section 2.1 this is a general phenomenon. There are, however, certain loopholes. For example, in the Wilson discretization of fermions, (2.13), a second-order derivative term $S_W$ which becomes irrelevant in the (naive) continuum limit was added to the naively discretized fermion action $S_F$. For the doubler fermions, this term generates a contribution to the mass which is proportional to $1/a$ so that they acquire infinite mass in the continuum limit $a \to 0$ and decouple. As this extra term couples left-handed to right-handed fermions chiral invariance is lost.

A number of proposals to overcome this difficulty have been suggested in the last few years. Quite generally, the situation is rather complex. For each model which typically

depends on quite a few parameters one has to map out the phase diagram. A careful analysis of the usually rich phase structure is then necessary to locate the region(s) in parameter space where a sensible continuum limit can be taken. All this requires a lot of numerical and analytical work and we cannot even attempt to present a comprehensive overview over all the results obtained so far. The material is discussed in much greater detail in recent reviews (De and Jersak 1992, Montvay 1992) to which we refer also for a more complete and fair list of references. Here we can only sketch some basic ideas and difficulties in this field.

A rather intensively investigated approach to chiral fermions on the lattice is the Smit–Swift model (Smit 1980, 1986, Swift 1984). The action of this model consists of a standard Higgs part $S_H$ (the lattice equivalent to (5.1)), the naive fermion action $S_F$ (2.13), a Yukawa term $S_Y$ plus a so-called Wilson–Yukawa part $S_{WY}$:

$$S = S_H + S_F + S_Y + S_{WY} \tag{5.8}$$

with

$$\begin{aligned} S_Y &= y \sum_n \{\bar{\psi}_L(n)\phi(n)\psi_R(x) + \mathrm{HC}\} \\ S_{WY} &= \frac{w}{2} \sum_n \{2\bar{\psi}_L(n)\phi(n)\psi_R(n) \\ &\quad - \bar{\psi}_L(n)\phi(n)\psi_R(n+\hat{\mu}) - \bar{\psi}_L(n+\mu)\phi(n+\hat{\mu})\psi_R(n) + \mathrm{HC}\} \end{aligned} \tag{5.9}$$

Here, $\psi_{L,R}$ denote the chiral projections $\frac{1}{2}(1 \mp \gamma_5)\psi$. The action is invariant under the global chiral $SU(2)_L \times SU(2)_R$ transformations

$$\begin{aligned} &\psi_L \to \Omega_L\psi_L, \bar{\psi}_L \to \bar{\psi}_L\Omega_L^\dagger \\ &\psi_R \to \Omega_R\psi_R, \bar{\psi}_R \to \bar{\psi}_R\Omega_R^\dagger \\ &\phi \to \Omega_L\phi\Omega_R^\dagger \end{aligned} \tag{5.10}$$

where $\Omega_L \in SU(2)_L$ and $\Omega_R \in SU(2)_R$†. The $SU(2)_L$ symmetry group is to be gauged later in order to make contact with the standard model. First of all, one has to deal with the doubler fermions half of which come with the opposite 'mirror' behaviour under chiral transformations. By analysing the fermion propagator it could be shown that at strong Wilson–Yukawa coupling $w$ the doublers acquire a mass which stays at order $1/a$ when the (bare) couplings are tuned to certain critical values, i.e. close to one of the second order phase transitions (Thornton 1989, Bock *et al* 1989, 1990b, Smit 1989, Golterman and Petcher 1990, Aoki *et al* 1990). Thus, there is a region in the space of parameters where the doublers are removed in the continuum limit. Still, the theory contains a right-handed neutrino as an elementary field. It could, however, be proved that at $y = 0$ the action possesses a shift symmetry in the right-handed fields (Golterman and Petcher 1989). Due to this symmetry the right-handed neutrino decouples, even when gauge interactions are switched on again. Both results had made the Smit–Swift model a promising candidate to investigate the standard model on the lattice. There is, however, a serious drawback. Apart

† The model has also been analysed with simpler symmetry groups such as e.g. $U(1)_L \times U(1)_R$.

from the elementary fields one has to analyse the spectrum of the model. In particular, there are composite mirror fields like $\phi^\dagger\psi_L$ which are left-handed but transform non-trivially under $SU(2)_R$. The propagation of such composite fermion operators has been looked at and the corresponding masses have been determined (Bock and De 1990, Bock *et al* 1992). It turns out that a Dirac fermion, $\phi^\dagger\psi_L + \psi_R$, which is neutral under $SU(2)_L$ but transforms vectorially under $SU(2)_R$ remains in the theory. This is of course not acceptable in the standard model.

As the presence of mirror fields apparently cannot be avoided, it has been suggested to include them as fundamental fields (Montvay 1987a,b). This proposal offers the opportunity of more flexibility and also of better control over the decoupling of mirror fermions. The fermion fields $\psi$ are supplemented by mirror fields $\chi$ such that $\chi_R$ transforms the same way as $\psi_L$. Then one can write chirally invariant mixed terms like $\psi_L\chi_R$ etc. The Wilson term is designed to offer the possibility of removing both fermion and mirror doublers,

$$\tilde{S}_W = \frac{r}{2}\sum_{n,\mu}\{2\bar{\psi}(n)\chi(n) - \bar{\psi}(n+\hat{\mu})\chi(n) - \bar{\psi}(n)\chi(n+\hat{\mu}) + (\psi \longleftrightarrow \chi)\}, \quad (5.11)$$

while there are separate Yukawa terms for $\psi$ and $\chi$

$$\begin{aligned}\tilde{S}_Y = {} & y_\psi \sum_n \{\bar{\psi}_L(n)\phi(n)\psi_R(n) + \mathrm{HC}\} \\ & + y_\chi \sum_n \{\bar{\chi}_L(n)\phi^\dagger(n)\chi_R(n) + \mathrm{HC}\}.\end{aligned} \quad (5.12)$$

In addition, a mixed bare mass term $\Sigma_n m\{\bar{\psi}(n)\chi(n) + \mathrm{HC}\}$ is present but no Wilson–Yukawa part. The model has mainly been investigated for a global chiral $U(1)_L \times U(1)_R$ symmetry. There are more free parameters than in the Smit–Swift model so that mapping out the phase diagram is even more demanding. Still, numerical results indicate that the doublers can be decoupled (Lin *et al* 1990, 1991a, Farakos *et al* 1991). However, the Dirac fields $\psi_A = \psi_L + \chi_R$ and $\psi_B = \psi_R + \chi_L$ transform non-trivially only under $U(1)_L$ and $U(1)_R$ respectively in the symmetric phase, which is completely vector-like when written in those fields, while in the broken phase they transform equally. Moreover, the shift symmetry is of no help when gauge interactions are turned on so that presumably the mirror fermions do not decouple. The real question is therefore to what extent the degeneracy between fermions and mirror fermions can be lifted in the broken phase in order not to come into conflict with phenomenology. This again requires careful investigations in various regions of parameter space, a formidable numerical task when it is attempted to derive quantitative results. There are indications that by a fine tuning of parameters the ratio of mirror fermion mass to the Higgs condensate, $m/\langle\phi\rangle$, can be made as large as 6, corresponding to a mirror fermion mass in the TeV range (Lin *et al* 1991b). Still, the properties of the model in the symmetric phase are probably not satisfactory for an understanding of symmetry breaking in theories with chiral fermions.

To end this section we mention two other approaches. In Borelli *et al* (1990) the formulation of a chiral gauge theory without mirror fermions is based on gauge fixing. The second proposal attempts to obtain chiral fermions as zero modes bound to a domain wall. This is generated, in five dimensions, by a mass term which depends on the extra dimension and which has the form of a kink (Kaplan 1992). The analysis of these ideas is not as advanced as in the Smit–Swift or the mirror model and it remains to be seen whether one can achieve a thorough understanding of the chiral sector of the standard model.

### *5.4. Strong-coupling QED*

QED is the best tested of all field theories and it describes, at currently explorable energy scales, the interactions of charged particles with remarkable precision. Yet, from perturbation theory it is known that for all finite values of the bare coupling the renormalized coupling goes to zero if the ultraviolet cut-off is sent to infinity—the so-called Landau pole. Even if this remains true for the exact solution, pure QED would still be a useful low-energy effective theory. However, at large energies the effective charge becomes large so that perturbation theory should not be trusted anymore. It is therefore possible that through non-perturbative effects the Callan–Symanzik β-function acquires an ultraviolet stable fixed point at which the theory could develop non-trivial new physics. For pure QED this problem might be regarded as academic, as the cut-off can be pushed to values beyond the Planck scale where QED should not be considered in isolation anyway. Nevertheless, in the context of more general models non-perturbative phenomena of non-asymptotically free theories may play an important role and QED provides a useful laboratory to study those effects.

A renewed interest in non-perturbative studies of QED arose after an investigation of the truncated Schwinger–Dyson equation for the fermion propagator revealed a continuous chiral phase transition, with chiral symmetry being broken spontaneously at strong coupling (Miransky 1985). Although the calculation did not include vacuum polarization effects it was argued that the critical coupling should be regarded as an ultraviolet stable fixed point at which the theory admits a non-trivial continuum limit. The existence of a chiral transition was confirmed by numerical studies of non-compact lattice QED (Kogut *et al* 1988, 1989). These lattice investigations also claimed to find support for a non-trivial critical behaviour. Later on, however, it was found (Booth *et al* 1989, Horowitz 1990, Göckeler *et al* 1990a) that, at least for four flavours, the critical exponents are consistent with mean field behaviour. In particular, the numerical computation of the Callan–Symanzik β function for the renormalized charge (Göckeler *et al* 1990b) showed that the charge matches to one-loop renormalized perturbation theory and vanishes in the continuum limit. In the matter sector, the scaling behaviour was also found to be consistent with triviality (Göckeler *et al* 1992). This corresponds to a large anomalous dimension for the chiral condensate, $\gamma_{\bar{\chi}\chi} = -2$, which also indicates renormalizability of a four-fermion interaction (Booth *et al* 1989). Analytically, these observations are supported by studies of a coupled set of Schwinger–Dyson equations which include certain effects of fermion loops (Rakow 1991, Kondo 1991). These and accompanying results suggest that the chiral transition of QED and of the Nambu-Jona Lasinio model are in the same universality class (Horowitz 1990).

It must be said, however, that these findings are not yet completely settled. The main issues being debated are the exact form of the scaling laws (Kocic *et al* 1993a), a problem which will require a large computational effort to be unambiguously clarified, and the occurrence (Kocic *et al* 1992, Hands *et al* 1992, Kocic *et al* 1993b) or not (Rakow 1993) of a monopole phase transition. If the chiral transition is driven by monopole condensation it would be a lattice artifact. Otherwise, in view of the large anomalous dimensions being observed, it may be concluded that non-asymptotically free theories can possess interesting new features not covered by perturbation theory.

## 6. Outlook

Numerical simulations on space-time lattices to date offer the most promising prospects to analyse non-perturbative phenomena in the standard model of electro-weak and strong interactions and beyond. In this review we have presented in some detail the numerical

techniques which have been developed over the last ten years and which are now being applied in large scale numerical calculations. For basic questions like the QCD mass spectrum or the heavy quark potential these calculations provide answers, which can and have successfully been compared with existing experimental data. Other calculations like those for the QCD phase transition or the weak matrix elements will in the near future reach an accuracy where they can make predictions for new experiments.

Nevertheless, there are open questions within the standard model which could not yet be addressed satisfactorily by present day methods. For instance, in questions like the role of $\Theta$-vacua or QCD at non-vanishing baryon number density one is led to path integrals with complex actions. So far no satisfactory algorithm has been found for such problems (for a review see e.g. Barbour 1992). The analysis of the electro-weak sector is still incomplete. One has not yet succeeded in developing a convincing formulation of chiral fermions on the lattice. New suggestions still have to be explored. In this sector, there is also considerable interest in understanding the temperature dependence of baryon number violating processes, which play a central role in the generation of a baryon number asymmetry during the electro-weak phase transition (for a recent review see e.g. Shaposhnikov 1992).

The study of the gravitational force or, more generally, string models on the lattice has not been mentioned by us at all. Here one usually follows quite a different approach. Rather than formulating the theory on a rigid hypercubic lattice one constructs dynamically triangulated lattices, which define random surfaces (for a recent review see e.g. Kawai 1992). Present investigations concentrate on understanding the phase structure of random surface models and on the identification of critical points at which a continuum limit can be taken. Not surprising, also here the inclusion of fermions is of central interest.

In the future, we expect that the numerical analysis of quantum field theories will even more so be a valuable tool to study quantitatively non-perturbative aspects of these theories, which otherwise would not be accessible. Although the analysis of many questions of interest is still limited by the available computer resources progress in QCD will be investigated on massively parallel computers, which will deliver more than $10^{12}$ floating point operations per second (Teraflops). This will exceed the presently available resources for typical QCD-projects by two orders of magnitude. Parallel to these hardware improvements the algorithms used in the simulation of quantum field theories have much improved. One thus can expect that in the future numerical techniques will be applied to questions which up to now are considered to be too difficult (Parisi 1992) computationally.

## Acknowledgments

We wish to thank Sourendu Gupta, U Heller, R Horsley, M Laursen and Th Neuhaus for discussions and for providing material for the preparation of this article. This work was partially supported by the DFG under grant PE 340/3-1.

## References

Abada A *et al* 1992 *Nucl. Phys.* B **376** 172
Adler S L 1981 *Phys. Rev.* D **23** 2901
Adler J *et al* (MARK III Collaboration) 1989 *Phys. Rev. Lett.* **62** 1821
Albanese M *et al* (APE Collaboration) 1987) *Phys. Lett.* **192B** 163
Alexandrou C 1991 *Phys. Lett.* **256B** 60
Allton C R *et al* 1991 *Nucl. Phys.* B **349** 598

—— (UKQCD Collaboration) 1992a *Phys. Lett.* **284B** 377
—— (UKQCD Collaboration) 1992b *Phys. Lett.* **292B** 408
Altmeyer R *et al* ($MT_c$ Collaboration) 1993 *Nucl. Phys.* B **389** 445
Alvarez O 1981 *Phys. Rev.* D **24** 440
Anjos J *et al* (E691 Collaboration) 1989 *Phys. Rev. Lett.* **62** 1587
—— 1990 *Phys. Rev. Lett.* **65** 2630
Aoki S *et al* 1990 *Phys. Lett.* **243B** 403
Appelquist T and Pisarski R D 1981 *Phys. Rev.* D **23** 2305
Bacilieri P *et al* (APE Collaboration) 1988 *Phys. Rev. Lett.* **61** 1545
Bali G and Schilling K 1992 *Phys. Rev.* D **46** 2636
—— 1993 *Phys. Rev.* D **47** 661
Barbour I 1992 *Nucl. Phys.* (*Proc. Suppl.*) B **26** 22
Batrouni G G *et al* 1985 *Phys. Rev.* D **32** 2736
Bernard C 1974 *Phys. Rev.* D **9** 3312
Bernard C *et al* 1988 *Phys. Rev.* D **38** 3540
Bernard C and Soni A 1990 *Nucl. Phys.* (*Proc. Suppl.*) B **17** 495
Bernard C *et al* 1991 *Phys. Rev.* D **43** 2140
—— 1992a *Phys. Rev.* D **45** 869
—— 1992b *Nucl. Phys.* (*Proc. Suppl.*) B **26** 204
—— 1992c *Nucl. Phys.* (*Proc. Suppl.*) B **26** 262
—— 1992d *Nucl. Phys.* (*Proc. Suppl.*) B **26** 305
—— 1992e*Phys. Rev. Lett.* **68** 2125
—— 1992f *Preprint AZPH-TH/92-16*
—— 1993 *Nucl-Phys. (Proc. Suppl.)* B **30** 465
Bhanot G *et al* 1990 *Nucl. Phys.* B **353** 551
Billoire A 1980 *Phys. Lett.* **92B** 343
Billoire A *et al* 1985 *Nucl. Phys.* B **251** 581
Binder K 1979 *Monte Carlo Methods in Statistical Physics* (Berlin: Springer)
Bitar K M *et al* (HEMCGC Collaboration) 1990a *Phys. Rev.* D **42** 3794
—— 1990b *Phys. Lett.* **234B** 333
—— 1991 *Phys. Rev.* D **43** 2396
—— 1993 *Nucl. Phys. (Proc. Suppl.)* B **30** 401
Bock W *et al* 1989 *Phys. Lett.* **232B** 486
Bock W and De A K 1990 *Phys. Lett.* **245B** 207
Bock W *et al* 1990a *Phys. Rev.* D **41** 2573
—— 1990b *Nucl. Phys.* B **344** 207
—— 1992 *Nucl. Phys.* B **388** 243
Booth S *et al* 1989 *Phys. Lett.* **228B** 115
—— (UKQCD Collaboration) 1992 *Phys. Lett.* **294B** 385
Borelli A *et al* 1990 *Nucl. Phys.* B **333** 335
Borgs C 1985 *Nucl. Phys.* B **261** 455
Born K D *et al* ($MT_c$ Collaboration) 1991a *Nucl. Phys.* (*Proc. Suppl.*) B **20** 394
—— 1991b *Phys. Rev. Lett.* **67** 302
Boyd G *et al* 1992a *Nucl. Phys.* B **376** 199
—— 1992b *Nucl. Phys.* B **385** 481
Bowler K *et al* 1986 *Phys. Lett.* **179B** 375
Brown F R and Woch T J 1987 *Phys. Rev. Lett.* **58** 2394
Brown F R *et al* 1988 *Phys. Rev. Lett.* **61** 2058
—— 1990 *Phys. Rev. Lett.* **65** 2491
—— 1991 *Phys. Rev. Lett.* **67** 1062
Buchmüller W and Cooper S 1988 *High Energy Physics* ed A Ali and P Söding (Singapore: World Scientific)
Bunk B *et al* 1992 *Phys. Lett.* **284B** 371
Butler F *et al* (GF11 Collaboration) 1993 *Phys. Rev. Lett.* **70** 2849
Cabasino S *et al* (APE Collaboration) 1991 *Phys. Lett.* **258B** 202
Cabbibo N and Marinari E 1982 *Phys. Lett.* **119B** 387
Callaway D J E and Rahman A 1982 *Phys. Rev. Lett.* **49** 613
Campostrini M *et al* 1986 *Phys. Rev. Lett.* **57** 44
Campostrini M and Rossi P 1990 *Nucl. Phys.* B **329** 753
Caracciolo S *et al* 1992 *Preprint FSU-SCRI-92-65*

Christ N H 1990 *Proc. 8th Conf. on Computing in High Energy Physics (Santa Fe)*
Coleman S and Weinberg E 1973 *Phys. Rev.* D 7 1888
Creutz M 1980 *Phys. Rev.* D **21** 2308
—— 1987 *Phys. Rev.* D **36** 515
—— 1988 *Phys. Rev.* D **38** 1228
Creutz M (ed) 1992 *Quantum Field Theory on the Computer* (Advanced Series on Directions in High Energy Physics) (Singapore: World Scientific)
Creutz M *et al* 1979 *Phys. Rev. Lett.* **42** 1390
Damgaard P H and Heller U M 1988 *Nucl. Phys.* B **304** 63
Daniel D *et al* 1992 *Phys. Rev.* D **46** 3130
Dashen R and Neuberger H 1983 *Phys. Rev. Lett.* **50** 1897
De A K and Jersak J 1992 *Heavy Flavours* ed A J Buras and M Lindner (Singapore: World Scientific)
DeTar C 1988 *Phys. Rev.* D **37** 2328
DeTar C and Kogut J 1987a *Phys. Rev. Lett.* **59** 399
—— 1987b *Phys. Rev.* D **36** 2828
Dine M *et al* 1992 *Phys. Rev.* D **46** 550
Drouffe J M and Itzykson C 1978 *Phys. Rep.* **38** 133
Duane S *et al* 1987 *Phys. Lett.* **195B** 216
Eichten E 1988 *Nucl. Phys.* (*Proc. Suppl.*) B **4** 70
Eichten E *et al* 1975 *Phys. Rev. Lett.* **34** 369
Eichten E and Feinberg F 1981 *Phys. Rev.* D **23** 2724
El-Khadra A X 1992 *Nucl. Phys.* (*Proc. Suppl.*) B **26** 372
El-Khadra A X *et al* 1992 *Phys. Rev. Lett.* **69** 729
Engels J *et al* 1990a *Phys. Lett.* **252B** 625
—— 1990b *Nucl. Phys.* B **332** 737
Evertz H G *et al* 1987 *Nucl. Phys.* B **285** 229
Farakos K *et al* 1991 *Nucl. Phys.* B **350** 474
Fingberg J *et al* 1993 *Nucl. Phys.* B **392** 493
Fischler W 1977 *Nucl. Phys.* B **129** 157
Fucito F *et al* 1981 *Nucl. Phys.* B **180** 369
Fukugita M and Ukawa A 1985 *Phys. Rev. Lett.* **55** 1854
Fukugita M *et al* 1986 *Phys. Rev. Lett.* **57** 1974
—— 1989 *Phys. Rev. Lett.* **63** 1768
—— 1990 *Nucl. Phys.* B **337** 181
—— 1992a *Nucl. Phys.* (*Proc. Suppl.*) B **26** 284
—— 1992b *Nucl. Phys.* (*Proc. Suppl.*) B **26** 265
—— 1993 *Phys. Rev.* D **47** 4739
Gasser J and Leutwyler H 1982 *Phys. Rep.* **87** 77
Gavai R V *et al* 1990 *Phys. Lett.* **241B** 567
—— 1992 *Phys. Lett.* **294B** 84
Gavela M B *et al* 1988a *Phys. Lett.* **206B** 113
—— 1988b *Nucl. Phys.* b **306** 677
Göckeler M *et al* 1990a *Nucl. Phys.* B **334** 527
—— 1990b *Phys. Lett.* **251B** 567
—— 1992 *Nucl. Phys.* B **371** 713
—— 1993 *Nucl. Phys.* B **404** 517
Goltermann M F L and Petcher D N 1989 *Phys. Lett.* **225B** 159
—— 1990 *Phys. Lett.* **247B** 370
Gottlieb S *et al* 1987a *Phys. Rev.* D **35** 2531
—— 1987b *Phys. Rev. Lett.* **59** 1881
—— 1988a *Phys. Rev.* D **38** 2245
—— 1988b *Phys. Rev.* D **38** 2888
—— 1992 *Nucl. Phys.* (*Proc. Suppl.*) B **26** 308
Gromes D 1984 *Z. Phys.* C **26** 401
Guagnelli M *et al* (APE Collaboration) 1990 *Phys. Lett.* **240B** 188
—— 1992 *Nucl. Phys.* **378B** 616
Gupta R *et al* 1986 *Phys. Rev. Lett.* **57** 2621
—— 1988a *Phys. Lett.* **211B** 132
—— 1988b *Phys. Rev.* D **38** 1278

—— 1989 *Phys. Rev.* D **40** 2072
—— 1991a *Phys. Rev.* D **43** 2003
—— 1991b *Phys. Rev.* D **44** 3272
—— 1993 *Phys Rev.* D **47** 5113
Gupta S 1992a *Nucl. Phys.* B **370** 741
—— 1992b *Phys. Lett.* **288B** 171
Gupta S *et al* 1990 *Phys. Lett.* **242B** 437
Hands S J *et al* 1992 *Phys. Lett.* **289B** *400*
Hasenbusch M 1990 *Nucl. Phys.* B **333** 581
Hasenfratz A and Hasenfratz P 1986 *Phys. Rev.* D **34** 3160
Hasenfratz A *et al* 1987 *Phys. Lett.* **199B** 531
Hasenfratz A and Neuhaus T 1988 *Nucl. Phys.* B **297** 205
Hasenfratz A *et al* 1990 *Z. Phys.* C **46** 257
Hasenfratz P and Leutwyler H 1990 *Nucl. Phys.* B **343** 241
Hashimoto S and Saeki Y 1992 *Nucl. Phys.* (*Proc. Suppl.*) B **26** 381
Herrmann H J and Karsch F (eds) 1991 *Fermion Algorithms* (Singapore: World Scientific)
Horowitz A M 1990 *Phys. Lett.* **244B** 306
Horsley R *et al* 1989 *Nucl. Phys.* B **313** 377
Huntley A and Michael C 1987 *Nucl. Phys.* B **286** 211
Iwasaki Y *et al* (QCDPAX Collaboration) 1991 *Phys. Rev. Lett.* **67** 3343
—— 1992 *Phys. Rev.* D **46** 4657
—— 1993 *Nucl. Phys. (Proc. Suppl.)* B **30** 397
Jansen K and Seuferling P 1990 *Nucl. Phys.* B **343** 507
Kalkreuter T 1992 *Preprint DESY 92-158*
Kaplan D B 1992 *Phys. Lett.* **288B** 342
Kapusta J I 1979 *Nucl. Phys.* B **148** 461
Karsch F *et al* 1987 *Phys. Lett.* **188B** 353
—— 1988 *Z. Phys.* C **37** 617
Karsch F and Wyld H W 1988 *Phys. Lett.* **213B** 505
Kawai H 1992 *Nucl. Phys.* (*Proc. Suppl.*) B **26** 93
Kennedy A D and Pendleton B J 1990 *Nucl. Phys.* (*Proc. Suppl.*) B **20** 118
Kilcup G 1991 *Nucl. Phys.* (*Proc. Suppl.*) B **20** 417
Kirzhnits D A and Linde A D 1972 *Phys. Lett.* **42B** 471
Kocic A *et al* 1992 *Phys. Lett.* **289B** 400
—— 1993a *Nucl. Phys.* B **397** 451
—— 1993b *Nucl. Phys.* B **398** 405
Kodama K *et al* (E653 Collaboration) 1992 *Phys. Lett.* **286B** 187
Kogut J B and Susskind L 1975 *Phys. Rev.* D **11** 395
Kogut J B *et al* 1988 *Phys. Rev. Lett.* **60** 772
—— 1989 *Nucl. Phys.* B **317** 253, 271
—— 1991 *Phys. Rev.* D **44** 2869
Koller J and van Baal P 1988 *Nucl. Phys.* B **302** 1
Kondo K-I 1991 *Int. Workshop on Strong Coupling Gauge Theories and Beyond* (1990) ed T Muta and K Yamawaki (Singapore: World Scientific)
Kripfganz J 1992 *Dynamics of First Order Phase Transitions* ed H J Herrmann, W Janke and F Karsch (Singapore: World Scientific)
Kühn J H and Zerwas P M 1988 *Phys. Rep.* **167** 321
Kuti J *et al* 1988 *Phys. Rev. Lett.* **61** 678
Lacock P *et al* 1992 *Nucl. Phys.* B **369** 501
Laermann E *et al* ($MT_c$ Collaboration) 1992 *Nucl. Phys.* (*Proc. Suppl.*) B **26** 268
Landsman N P 1988 *Nucl. Phys.* B **322** 498
Langhammer F 1986 *Diplomarbeit RWTH Aachen*
Langguth W and Montvay I 1987 *Z. Phys.* C **36** 725
Lee B W *et al* 1977 *Phys. Rev.* D **16** 1519
Lepage P and Mackenzie P 1993 *Phys. Rev.* D **48** 2250
Lin L *et al* 1990 *Z. Phys.* C **48** 355
—— 1991a *Phys. Lett.* **264B** 407
—— 1991b *Nucl. Phys.* B **355** 511
Linde A D 1980 *Phys. Lett.* **96B** 289

Lombardo M-P *et al* 1993 *Nucl. Phys.* B **395** 388
Lüscher M *et al* 1980 *Nucl. Phys.* B **173** 365
Lüscher M and Weisz P 1987 *Nucl. Phys.* B **290** 25
—— 1988 *Nucl. Phys.* B **295** 65
—— 1989 *Nucl. Phys.* B **318** 705
Lüscher M *et al* 1993 *Nucl. Phys.* B **389** 247
Lubicz V *et al* 1991 *Nucl. Phys.* B **356** 301
—— 1992 *Phys. Lett.* **274B** 415
Maiani L and Testa M 1990 *Phys. Lett.* **245B** 585
Manousakis E and Polonyi J 1987 *Phys. Rev. Lett.* **58** 847
Marinari E 1993 *Nucl. Phys. (Proc. Suppl.)* B **30** 122
Martinelli G *et al* 1991 *Nucl. Phys.* B **358** 211
—— 1992 *Nucl. Phys.* B **378** 591
Matsui T and Satz H 1986 *Phys. Lett.* **178B** 416
Mawhinney R 1993 *Nucl. Phys. (Proc. Suppl.)* B **30** 331
Metropolis N *et al* 1953 *J. Chem. Phys.* **21** 1087
Michael C 1992 *Phys. Lett.* **283B** 103
Michael C and Teper M 1989 *Nucl. Phys.* B **314** 347
Miransky V A 1985 *Nuovo Cimento* **90A** 149
Montvay I 1987a *Phys. Lett.* **199B** 89
—— 1987b *Phys. Lett.* **205B** 315
—— 1992 *Nucl. Phys. (Proc. Suppl.)* B **26** 57
Negele J 1993 *Nucl. Phys. (Proc. Suppl.)* B **30** 295
Neuberger H 1988 *Nucl. Phys.* B **300** 180
Nielsen H R and Ninomiya M 1981 *Nucl. Phys.* B **193** 173
Parisi G 1980 *Proc. XXth Conf. on High Energy Physics (Madison, WI)*
—— 1992 *Nucl. Phys. (Proc. Suppl.)* B **26** 181
Parisi G and Wu Y S 1981 *Sci. Sin* **24** 483
Patrascioiu A and Seiler E 1992 *Preprint MPI-Ph/92-18, LPTHE 92/63*
Petcher D N and Weingarten D H 1981 *Phys. Lett.* **99B** 333
Petersson B 1993 *Nucl. Phys. (Proc. Suppl.)* B **30** 66
Pisarski R D and Wilczek F 1984 *Phys. Rev.* D **29** 338
Polyakov A M 1979 *Phys. Lett.* **82B** 2410
Rakow P E L 1991 *Nucl. Phys.* B **356** 27
Rakow P E L 1993 *Nucl. Phys. (Proc. Suppl.)* B **30** 591
Rebbi C (ed) 1983 *Lattice Gauge Theories and Monte Carlo Simulations* (Singapore: World Scientific)
Reisz T 1991 *J. Math. Phys.* **32** 115
—— 1992 *Z. Phys.* **53** 169
Scalettar R T *et al* 1986 *Phys. Rev.* B **34** 7911
Sexton J C and Weingarten D H 1992 *Nucl. Phys.* B **380** 665
Shaposhnikov M 1992 *Nucl. Phys. (Proc. Suppl.)* B **26** 78
Sharatchandra H S *et al* 1981 *Nucl. Phys.* B **192** 205
Sharpe S *et al* 1992a *Nucl. Phys.* B **383** 309
—— 1992b *Nucl. Phys. (Proc. Suppl.)* B **26** 197
Sheikoleslami B and Wohlert R 1985 *Nucl. Phys.* B **259** 572
Smit J 1980 *Nucl. Phys.* B **175** 307
—— 1986 *Acta Phys. Polon.* B **17** 531
—— 1989 *Nucl. Phys. (Proc. Suppl.)* B **9** 579
Svetitsky B and Yaffe L G 1982a *Phys. Rev.* D **26** 963
—— 1982b *Nucl. Phys.* B **210** 423
Swendsen R H and Wang J-S 1987 *Phys. Rev. Lett.* **58** 86
Swift P V D 1984 *Phys. Lett.* **145B** 256
Symanzik K 1983a *Nucl. Phys.* B **226** 187
—— 1983b *Nucl. Phys.* B **226** 205
Teper M 1986 *Phys. Lett.* **183B** 345
Thornton A M 1989 *Phys. Lett.* **221B** 151
Unger L 1992 *Preprint CU-TP-571*
van Baal P and Kronfeld A 1989 *Nucl. Phys. (Proc. Suppl.)* B **9** 227
Vohwinkel C 1989 *Phys. Rev. Lett.* **63** 2544

Weinberg S 1974 *Phys. Rev.* D **9** 3320
Weisz P 1981 *Phys. Lett.* **100B** 331
Wilczek F 1992 *Int. J. Mod. Phys.* A **7** 3911
Wilson K 1974 *Phys. Rev.* D **10** 2445
Wolff U 1989 *Nucl. Phys.* B **322** 759